United States Naval Postgraduate School

THESIS

A NEW OPTIMIZATION THEORY FOR THE END-INITIATED LINEAR SHAPED CHARGE

by

George Elliott Brown, Jr.

October 1969

This document has been approved for public release and sale; its distribution is unlimited.

A New Optimization Theory for the End-Initiated Linear Shaped Charge

by

George Elliott Brown, Jr.
Lieutenant, United States Navy
B.S.U.S., Naval Academy, 1962

Submitted in partial fulfillment of the requirements for the degree of

MASTER OF SCIENCE IN AERONAUTICAL ENGINEERING

from the

NAVAL POSTGRADUATE SCHOOL
October 1969

Author _____

Approved by: _____
Thesis Advisor

_____
Chairman, Department of Aeronautics

_____
Academic Dean

ABSTRACT

An exposition of the two existing analytical approaches to the end-initiated linear shaped charge is made. After a theory is put forth relating optimization to increased energy transfer at increased standoff distances, this effect is linked to the dispersive nature of the jet mass. An analytical design approach is then formulated that combines elements of both existing models. The object of this approach is to integrate experimental data into a mathematically definitive analysis. A theoretical link is then developed between the dispersive nature of the jet and the design input parameters, thus completing the optimization model.

TABLE OF CONTENTS

LIST OF ILLUSTRATIONS

TABLE OF SYMBOLS

V_D	Velocity of the detonation wavefront
$\bar{X}\bar{Y}\bar{Z}$	Inertial coordinate system
η,ζ,ξ	Coordinate system that is translating with the detonation front
η^*,ζ^*,ξ	Mirrored translating coordinates that define the "other" liner wall
t	time measured from initiation of charge
t'	time for a fixed point in the charge, measured from passage of detonation wave
T	the total time required for the detonation wave to traverse the charge length L
θ	half the included angle of the "V" trough
Θ	half the included angle of the star point
S	the label for a general streamline
S^*	the label for the streamline symmetric to S
C	the label for the curve of impact
P	the point of impact of S and S^*
ξ_C,ζ_C	coordinates of the impact curve C
ξ_C,Z_C	coordinates of the impact curve C
$KE_j(KE_{SL})$	Relative Kinetic Energy of the jet (slug)
$M_j(M_{SL})$	Relative Mass of the jet (slug)
L	Length of Charge
$V_j(V_{SL})$	Velocity of the jet (slug) particle in the translating frame
$\hat{V}_j(\hat{V}_{SL})$	Inertial velocity of the jet (slug) particle
V_P	Projection of incident liner velocity in the plane of symmetry

u_p	component of V_p in ξ direction
w_p	component of v_p in Z direction
i_p	included angle of S and S^*
ϕ_p	angle between v_p and ξ axis
α_C	angle between local tangent to C and ξ axis
σ	spray angle associated with a particular streamline
$\mu_j(\mu_{SL})$	the area mass density of the jet (slug) at a point
t_r	Reverberation time or time required for the stress wave to traverse twice the liner width
T_R	Relief time - a constant accounting for the detonation front curvature and release wave velocity for a particular charge configuration
M_L	Mass of the liner
$\bar{\eta}$	coordinate measured with reverse sign along η from a zero at η_{max}

ACKNOWLEDGEMENTS

The author wishes to express his grateful thanks to Professor J. E. Sinclair, his advisor, to Dr. R. G. S. Sewell who was a constant source of encouragement and to Asst. Professor D. W. Netzer for his timely advice.

1. INTRODUCTION

The end-initiated linear shaped charge is a fairly recent application in the warheads field. Essentially it is a refinement of the basic phenomenon of shaped or cavity charges first discovered by Monroe in 1888. Although the same principle of end-wave initiation is used in linear metal cutting charges for such applications as stage separation in rocketry, nowhere is the efficiency of the mechanism as important as in the warhead application. The immense cost of maintaining and exercising today's delivery systems, measured in dollar value or by other means, dictates great marginal utility for any improvement in warhead effectiveness. Such an improvement in effectiveness is difficult to measure and usually not a function of size. It is best described as achievement of a better compromise. The trend in recent years has been to match specific type targets to specially designed warheads such as the linear shaped charge but this entails an undesirable loss of employment flexibility. An improvement in the effectiveness of this type of warhead therefore must pertain to all types of targets and must increase the effective radius in order to cut down on the number of weapons that must be delivered to the target area to insure it's destruction.

II. THE END-INITIATED LINEAR SHAPED CHARGE

The basic mechanism of the end-initiated linear shaped charge (hereinafter referred to simply as LSC) is so complex as to defeat any purely mathematical approach to it's description. Moreover, its action is so catastrophic in nature that it obviates many of the empirical analysis techniques used to unlock the secrets of other pressure-time dependent phenomena. A much simplified description of the basic mechanism of jet and slug formation is a necessary background for understanding of the analytical model of the LSC.

The simplest configuration of the LSC is that of Figure 1, a long column of solid explosive which has had a "V" notch inscribed in one of it's surfaces. The interior of this notch is lined with a layer of metal such as copper, aluminum, or mild steel. In operation the explosive column is initiated at one end resulting in the steady-state detonation condition where the detonation wave (a planar wavefront perpendicular to the charge axis in our simple case) is propagating down the column axis at a constant detonation velocity V_D. The peak pressure pulse whose leading edge is coincident with (indeed the triggering mechanism of) the detonation wave begins to deform the metal liner upon its passage. As the two sides of the "V" are "squeezed" together, symmetric elements of each wall collide and separate such that the liner as a whole is divided into

two fairly distinct masses, both of which propagate away from the charge axis in the longitudinal plane of symmetry of the "V" notch. These masses are commonly termed the jet and the slug [Figure 2]. The jet consists of a thin sheet of molten liner material with particle velocities on the order of 15,000 ft./sec., while the slug tends to be less discrete in the propagation plane and possesses particle velocities in the 5,000 ft./sec. range.

The damage-producing potential of even a small mass of material at jet velocities is quite evident, but the jet and slug have another characteristic that is very important in their ability to cut metal or to retain their energy over moderate distances. The jet is dispersive in nature. That is, the leading edge particles of the jet are possessed of initial velocities considerably in excess of those of the trailing edge. Thus, the jet sheet stretches longitudinally (radially with respect to the original charge axis) as it propagates. Conversely, the slug's leading edge has a lower initial velocity than its trailing edge and thus, it tends to coalesce as it propagates. These important properties will be examined in greater detail in Section IV.

The included angle of the notch (2θ) must, of course, lie between 0° and 180°. We see in Figure 3, however, that when we combine several charges into the cylindrical container required of most warhead applications, we further restrict the "V" angle. In the illustrated case of eight propagation planes, a θ value of 22½° would leave no

interior volume for the required explosive. For ease in understanding, this configuration with $2\theta = 120°$, and the star point angle $2\theta = 75°$ is used as the point of departure throughout this thesis.

III. THEORETICAL BACKGROUND

There are in existence two analytical approaches to the end-initiated linear shaped charge. By far the most rigorous from a mathematical viewpoint is the analytical model of M. A. Garcia contained in Reference 2. This model treats the LSC mechanism in detail through jet and slug formation. The other extant formulation is that of Robert G. S. Sewell [Reference 1]. Here a building block approach is used in an effort to separate the effects of the significant parameters and a great deal more correlation with empirical results is made. Both of these treatments constitute the foundation of this thesis. In the interests of continuity, the terminology of the more mathematical Reference 2 will be used wherever possible. Following Garcia, then, an inertial coordinate frame, (X,Y,Z in Fig. 4) fixed to the charge which in turn is fixed in space established. The X axis is coincident with the trough apex, with the origin at the initiator end, and the X-Z plane defining the plane of symmetry of the trough.

Two important basic assumptions, germane to the entire analysis, are now made.

Assumption #1. The detonation wavefront propagates through the explosive longitudinally at a constant velocity. End effects are neglected and only steady-state jetting is considered. This assumption holds throughout this thesis.

Assumption #2. The detonation wavefront is contained in a plane perpendicular to the charge axis and moving in the positive X direction at velocity V_D. This assumption holds throughout the analysis of Garcia, and in part of Sewell's study, but is further examined in Section V of this thesis. Armed with these assumptions, a moving coordinate frame (η,ζ,ξ) whose origin at any one time is defined by the intersection of the detonation front and the X axis is defined. The ξ axis is coincident with the X axis, but directed back toward the origin of the inertial X,Y,Z system. The η-ζ plane defines the detonation front with the η axis lying in the plane of one liner wall [Figures 4 and 5].

Assumption #3. The solid metal liner is treated as an incompressible, inviscid fluid with no internal stress and in a steady flow state, the flow velocity being a constant V_D to an observer riding the η,ζ,ξ coordinate frame. Garcia's basis for this is the extreme pressure (on the order of 200 to 300 kilobars) and temperatures existing behind the blast wave, as well as the detonation velocity which is in the neighborhood of 25,000 ft./sec. for a representative explosive composition. This assumption is also re-examined in Section V.

Assumption #4. The pressure forces behind the deforming liner act along the normal to the η-ξ plane and the deviation of the deforming liner in the ζ direction is small.

This assumption also receives more attention later in the development.

Assumption #5. Liner particles do not change their η values until they reach the curve of impact C in the plane of symmetry. Thus, each η value defines a streamline (S) continuous in both the undisturbed and deforming portions of the liner. Now another coordinate system (η^*,ζ^*,ξ, the mirror image of η,ζ,ξ) can be introduced to define symmetrical streamlines (S^*) in the other wall. It can now be seen in Figure 6 that "fluid" particles of values $\eta=\eta^*$ and X=X travel respectively along streamlines S and S^* to eventual collision at a point P on the curve of impact in the plane of symmetry.

Assumption #6. Kinetic energy, total mass, and momentum in the plane of symmetry are conserved in the particle impacts at point P. Thus, due to symmetry and this lossless assumption, each particle of liner reacts as if it were impacting a solid frictionless wall coincident with the plane of symmetry.

Proceeding on the basis of the above assumptions, it can be determined that, upon reaching the curve of impact, the liner particles separate into jet and slug through a collision process entirely within the plane of symmetry. Thus, two dimensional vector equations can be written in the symmetry plane for the components of velocity

$$\left.\begin{aligned} (1) \qquad \vec{V}_j &= u_j \vec{e}_\xi + \dot{z}_j \vec{e}_z \\ (2) \qquad \vec{V}_{SL} &= u_{SL} \vec{e}_\xi + \dot{z}_{SL} \vec{e}_z \end{aligned}\right\} \text{ where } u = \dot{\xi}$$

These four velocity components, together with the two area mass densities at the curve of impact constitute the six unknowns of a complete description of the collision process. The area mass densities μ_j and μ_{SL} are defined by:

$$(3) \qquad dm_j = \mu_j dZ d\xi \quad \text{and} \quad dm_{SL} = \mu_{SL}\, dZ d\xi$$

The principles of conservation of kinetic energy, mass, and momentum introduced in assumption #6 provide five constraint equations, necessitating one further assumption. The following assumption, introduced by Garcia to render the problem determinate, is critical to the entire mathematical analysis.

Assumption #7. The streamline of the jet and slug form symmetrically with respect to the direction of flow of the liner streamline as projected in the plane of symmetry before impact. Figure 7, where V_p is the component of the incident liner streamline in the plane of symmetry, depicts this geometry.

As a result of Assumption #7 and the conservation relations Garcia proves that the spray angle σ is identically equal to the angle of incidence between the incoming line streamline and the plane of symmetry ($2\sigma = i_p$) [Figure 8].

This is an important concept and it is brought up again in Section V. It is also important to note that the slope of the curve of impact at any point P must exceed the slope of the incoming liner streamline projection in the symmetry plane. The flow geometry resulting from this consideration is portrayed in Figure 9.

The jet and slug velocities in the inertial frame may now be found by vector addition of the detonation wave velocity as depicted in Figure 10. Here, in the simple view for one liner streamline (one constant value of η and η^*), some characteristics noted experimentally show up. The jet exhibits a much greater velocity and about double the lead angle as compared to the slug material. Garcia goes on to develop the mathematical basis for the mapping of lines of constant η in the liner into their respective positions in the jet and the slug at any time $\frac{t}{T}$ by means of a Jacobian of transformation*. An example of the mapping for his most general case is presented as Figure 11.

The analytical model of Garcia then provides a precise means whereby, given the charge geometry, the detonation velocity and the profile of the pressure pulse, all of the pertinent jet and slug characteristics can be found. This is subject only to the assumptions delineated above. Although this model is a profound instrument for understanding the physics of the LSC, the fact that it hinges on intimate

---

*Here T is the time required for the detonation wave to traverse the entire charge.

knowledge of the pressure parameter renders it inadequate of itself for optimization techniques. Instrumentation capable of describing the extremes of the pressure pulse delivered by the blast wave in the explosive as a function of the charge surface coordinates is not likely to be available in the near future. Some means of equating charge performance with measurable parameters is essential to any charge effectiveness improvement program.

Considerable insight in this direction is provided by the pioneering work of R.G.S. Sewell contained in Reference 1. Here the method is to start with a simple two-dimensional description of jet and slug formation, and then to successively introduce the complexities necessary for a complete description, each couched in two-dimensional terms. A brief synopsis of this work is pertinent here. Sewell's development takes it's genesis in the case of two plates or liner sides being propelled along their respective normals (ζ and ζ^* axes) at a constant velocity ($\dot{\zeta} = \dot{\zeta}^* = \text{const.}$). Thus, as shown in Figure 12, the incidence angle θ is maintained as a constant. This, in fact, embodies the essence of Assumption #4 above. Making the assumption of conservation of kinetic energy, mass, and momentum (#6 above) and, in addition, applying the incompressible inviscid fluid assumption of #3, <u>but only at the point of collisions and beyond</u>, the following relationships result:

$$(4) \qquad M_j = \frac{1}{2} M_L (1 - \cos \theta)$$

$$(5) \qquad M_{SL} = \frac{1}{2} M_L (1 + \cos \theta)$$

$$(6) \qquad KE_j = \frac{1}{4} M_L \dot{\zeta}^2 (1 + \cos \theta)$$

$$(7) \qquad KE_{SL} = \frac{1}{4} M_L \dot{\zeta}^2 (1 - \cos \theta)$$

where KE = Kinetic energy per unit mass and $\dot{\zeta} = \dot{\zeta}^*$, and
M_L = mass of the liner

The balance between mass and kinetic energy of the slug and jet evident in the above equations is further amplified in Figure 13, a plot of $1 \pm \cos \theta$. In actuality only a portion of this plot is of practical interest, θ values less than about 30° and greater than 90° (flat plate) having no meaning in the analysis. Coincident with the mass and energy relations, the jet and slug velocities can similarly be expressed as functions of θ for the idealized case at hand.

$$(8) \qquad V_j = \dot{\zeta} (\csc \theta + \cot \theta)$$

$$(9) \qquad V_{SL} = \dot{\zeta} (\csc \theta - \cot \theta)$$

Using a $\dot{\zeta}$ value predicted by the Stern flat sandwich equations (References 3 and 4), Sewell shows that the above velocity equations correlate nicely with measured values (at the leading edge of the jet). The jet leading edge velocity is formed by collisions at the apex of the "V" trough, however, here the constant angle assumption is essentially met. The mass (and thus, also energy) balance

observed empirically does not, however, agree when taken for the whole charge. Sewell's next step introduces the effect of the variation in acceleration history across the wave, (from apex of trough to its edge). Taking a mean of the stepwise velocity functions caused by the reverberating shock wave in the plate and also accounting for the propagation of the release wave in the explosive products from the edge Sewell describes the velocity as:

$$(10) \qquad \dot{\zeta} = \dot{\zeta}_o \, (1 - e^{t/tr})$$

where t_r is the reverberation time, or the time required for the stress wave to traverse twice the liner thickness, and $\dot{\zeta}_o$ is again calculated by the Gurney-Stern formulas. Signifying η measured in a negative direction from a zero at the edge of the vane by $\bar{\eta}$, Sewell's function for displacement becomes:

$$(11) \qquad \zeta(\bar{\eta},t) = \dot{\zeta}_o \int_o^{T_R} (1 - e^{-t/tr}) \, dt + (t - T_R) \dot{\zeta} (1 - e^{-T_R/t_r})$$

where T_R, the relief time, is a correction factor for the release wave velocity and the curvature of the detonation front. Here the integral accounts for displacement during acceleration and the second term represents propagation at the constant initial velocity. Solutions to Equation 11 for various times after passage of the detonation front are presented in Figure 14. The figures are for a charge where η_{MAX} = 3 inches. Here the dotted line corresponds to the

plane of symmetry for an angle $\theta = 60^{\circ}$. The solution times are, of course, equivalent to various values of coordinate ξ in the translating frame. The effect of this displacement profile on the effective value of the trough angle (at successive ξ values on the curve of impact) is accentuated by the labeled tangents.

Sewell next accounts for the acceleration history longitudinally along the vane behind the detonation wave front. Here, again, the effect of stress wave reverberation makes itself felt on the displacement profile, but the release wave is not a factor. Figure 15 depicts the stress wave effect on the liner with area CDE representing a Prandtl-Meyer expansion. Sewell defines the instantaneous angle assumed by the disturbed liner with respect to its original position (here designated ω) as a function of time. Again the function is a continuous approximation to the discontinuous function resulting from the reverberation effect. Here:

$$(12) \qquad \omega(t) = \omega_o \left(1 - e^{-t/t_r}\right)$$

where ω_o is the final (maximum) angle assumed. This function is depicted in Figure 16 and, assuming a constant V_D, a simple re-labeling of the axes transforms the curve into a plot of ζ versus ξ (longitudinal acceleration effect only). Sewell then enters this effect into his model by tipping the previous solution through the angle ω_o. Note that this neglects the effect of curvature of the detonation

wavefron.. A velocity vector summation with representative midrange values for a charge similar to that depicted in Figure 3 is then performed [Figure 17]. These values correspond quite well with experimentally observed values of lead angle and mean velocity.

Comparison of Sewell's approach to the Garcia model yields several important differences. It is most significant that Sewell does not rely on the ideal fluid assumption (#3) until the impact that forms the jet and slug takes place. Garcia on the other hand treats the liner as inviscid and incompressible throughout its deformation by an impulsive overpressure and subsequent relief pressure. Further, the curvature of the detonation wavefront, only partly treated by Sewell, introduces extreme mathematical complexity into the Garcia model. The normal force assumption (#4) is common to both approaches as it is embodied in the Gurney and Sterne formulas used by Sewell. While Garcia's treatment is unique in providing a definable particle by particle analysis rather than a midrange value, it suffers from the dependence on experimentally unattainable pressure measurements as previously mentioned. Sewell's approach, on the other hand, furnishes an appealing dissection of the three-dimensional problem into two-dimensional displacement functions that show promise of experimental verification. In short, elements of both analyses are necessary for any attempt at charge performance improvement.

IV. APPROACH TO OPTIMIZATION THEORY

The first consideration in any optimization procedure must, of course, be some definition of its goals, preferably a direct measure of degree of optimality. Unfortunately the uses to which the shaped charge warhead is put, the conditions under which it is expected to perform it's task, and the variables involved in it's operation are far too diverse to allow any such precise measurement function. A great deal of attention has been given the target effects of shaped charge jets in recent years, particularly by the Ballistics Research Laboratory in regard to conical shaped charges. Some of the reports on this work, notably by DiPersio, Simon, and Merindino are listed as References 5 through 8. References 9 through 13 pertain more directly to the end-initiated LSC which has received emphasis at the Naval Weapons Center.

The original emphasis on shaped charge use was the localized defeat of armor plate in point attack by conical charges. The more recent use of the LSC reflects a shift in emphasis, utilizing the basic damage mechanism to inflict linear damage on softer metal targets, particularly steel and concrete bridge structures. Recently tactical commanders have stressed the need for weapons that afford as great a choice of target as possible. They stress this need for flexibility particularly in the case of air delivered

weapons. References 9, 11, and 13 then reflect effectiveness studies of an LSC warhead against targets such as missile sites, truck parks, and gun emplacements as well as bridge structures.

An optimization procedure, therefore, must lead to an increase in the warhead's effectiveness against the general target - "softer" for the most part and, significantly, more widely dispersed. This must be accomplished without degrading it's performance against girders and trusses at short range. A basic characteristic of shaped charge action must be sought, the control of which will provide increased weapon effectiveness against targets at greater "standoff" distances. That characteristic is the dispersive nature of the jet material mentioned previously. The selection of dispersion as the subject for optimization will now be justified.

Most of the studies made on the effectiveness of shaped charges pertain to the use of conical charges against armor targets. References 5 and 6 by DiPersio, et. al., show that penetration effects increase with increased standoff distance up to an optimum value and then drop off significantly. By means of flash radiographs (not reproducible here) they were able to correlate this optimum standoff distance with the maximum jet length before particulation*. As stated in Section II the dispersive velocity gradient

---

*Particulation refers to that point where the jet simultaneously fragments along its entire length.

from tip to tail of the jet causes the jet to stretch longitudinally during propagation. This continues until the limit of cohesion of the jet material is reached at which time the jet particulates into a string of elements. These elements are of fairly uniform lengths of the order of 2 - 5 times jet width at particulation and continue to lengthen thereafter. DiPersio and Simon's discovery that this particulation is instantaneous along the entire jet length is particularly significant. It led to their relation of penetration to jet break-up time depicted in Figure 18. Figure 19, also from Reference 7, relates hole volume to jet break-up time. In essence this figure shows that reducing the dispersive nature of the jet which, in turn, produces greater values of jet break-up time, results in a quantum jump in the efficiency of energy transfer from the charge to the target at <u>all</u> standoff ranges.

There is a limitation imposed, however, in that elimination of the dispersive gradient of the jet altogether would eliminate the mechanism by which the jet cuts metal targets. The gradient allows time for a jet particle to plastically react with a portion of the target mass by exceeding its dynamic yield strength and then flow away from the point of impingement before the arrival of the next jet particle. For this reason the retention of a small, but controlled gradient is probably advisable.

V. OPTIMIZATION THEORY

Armed with a specific charge parameter, namely dispersion, the control of which will produce the desired targeting effects, a basis for LSC optimization has been established. It remains to identify the physical aspects of the LSC that give birth to the dispersive effect of the jet and to link them to variables measurable by experimental means. Finally, one or more parameters that can control the dispersion and yet are capable of manipulation by the warhead designer must be isolated.

Some of the salient differences between the theories of Garcia and Sewell were highlighted at the end of Section III. It becomes apparent that reconciliation of the combined two-dimensional approach of Sewell with the translating reference frame and analytical description of impact kinetics of Garcia's description obviates many of their respective drawbacks to our purpose. The means of empirical verification and, if necessary, function description is introduced into Garcia's analysis by means of the longitudinal and lateral displacement profiles of Sewell's approach. In an attempt to probe the feasibility of such experimental identification of the displacement functions, and to gain insight into the magnitude of difference between the two original theories, a limited investigation was conducted. This investigation is outlined in Appendix A. The discontinuities in displacement and

velocity predicted at points C and H-J on Figure 15 were identifiable only on a statistical basis, but this is probably attributable to the quality of the data which was not generated for this particular investigation. The fact that a steady-state velocity is reached after approximately two reverberation times was verified. It is felt that careful analysis of experimental work done specifically for the purpose could successfully identify the required two-dimensional functional relationships.

The experimental work of Appendix A leads logically to a possible means of relating empirically definable functions to a theoretical formulation of shaped charge physics. A more sophisticated system than the one used in Appendix A should be able to define the acceleration history across the vane by description of the instantaneous displacement profile at various constant values of ξ. This will require a larger scale model initiated by a plane wave generator and probably utilization of flash radiography or betagraphy. The point to such a test program would be to isolate and mathematically describe the following physical functions:

1.) displacement function in the ζ-ξ plane (Appendix A)

2.) displacement function in the η-ζ plane

To these would be added the following functions over which the LSC designer has some control:

3.) detonation wave shape as a function in the η-ξ plane

4.) half angle of notch (θ)

Another design variable that could be added later if necessary is:

5.) shape of liner sides in the η-ζ plane

The above procedure reduces the problem of defining the convoluted surface, or the complex shape that is taken on by the liner between the detonation wavefront and the plane of symmetry, to a problem in solid geometry well within the capabilities of a modern third-generation computer. What remains is to define a parametric link between the dispersion of the jet elements and some aspect of this convoluted surface. We are led to a re-examination of the kinetics of impact in the plane of symmetry.

Garcia's critical assumption in this impact process (assumption #7) was that the jet and the slug form symmetrically with respect to the direction of flow of the liner streamline as projected in the plane of symmetry before impact. This leads to a prediction of equal amounts of liner mass going into the jet and slug, a conclusion that is not collaborated by experimental evidence. As pointed out by Garcia himself, unbalanced mass distributions are predicted only by streamline separations symmetrical to a line having steeper or shallower inclination than the projected streamline.

If we examine the conversion of the jet and slug velocities to the inertial frame, we see in Figure 20 that the locus of possible solutions to these inertial velocities

lie on a circle of radius V_D that is equivalent to that in the translating frame. Removing Garcia's restriction that the symmetrical streamline division be defined by V_p, we will replace V_p by an arbitrary direction that might be V_p, the local tangent to the curve of impact, or some unknown combination thereof. Continuing to denote the arbitrary vector's slope by ϕ as we did for V_p we combine the geometry in Figure 21. Since the inertial velocities form chords of the circular locus, we can express them as functions of the subtended angle. Using the cap (^) to denote inertial quantities, ...

$$(13) \qquad \hat{V}_j = 2\ V_D \sin\ (\frac{\phi+\sigma}{2})$$

$$(14) \qquad \hat{V}_{SL} = 2\ V_D \sin\ (\frac{\phi-\sigma}{2})$$

It has long been known, as noted previously, that elements of the jet exhibit a dispersive velocity gradient, and that the leading edge of the jet is formed at the apex of the notch. From these two facts it follows that:

$$(15) \qquad (\hat{V}_j)_\eta > (\hat{V}_j)_{\eta+\Delta\eta}$$

Combining equations 13 and 15 leads to:

$$(16) \qquad (V_D)_\eta \sin\ (\frac{\phi+\sigma}{2})_\eta > (V_D)_{\eta+\Delta\eta} \sin\ (\frac{\phi+\sigma}{2})_{\eta+\Delta\eta}$$

Any variation of V_D as a function of η would have to be due to variations in the velocity in the ζ (and ζ^*) directions. These variations are reflected in the convoluted

surface shape and, given the detonation velocity on the order of 25,000 ft./sec., are relatively minor. There doesn't seem to be much basis for a significant variation of V_D with η and this then leads to the conclusion that:

$$(17) \qquad (\phi+\sigma)_{\eta} > (\phi+\sigma)_{\eta+\Delta\eta}$$

Proceeding with an analagous development for the slug uncovers a discrepancy in the existing theory. Eichelberger, Pugh, and Rostoker (References 14 and 15) in their work with conical shaped charges uncovered the fact that there is a continuity in jet and slug formation in that the last formed jet element travels at the same speed as the last formed slug elements. A close examination of Garcia's work reveals that he assumes that both the jet and slug are dispersive. He further bases his work on the assumption that the trailing edge of the slug is formed at the apex of the notch. This leads to a satisfying balance of energies in that the highest velocity portion of the jet is being formed with the lowest velocity portion of the slug and vice versa.

The difficulty here is that recovered portions of the slug such as the cross-section shown in Figure 22, evidence a coalescent rather than a dispersive inception. Indeed, the very fact that the jet and slug have been recognized as separate entities since the earliest experiments strongly suggests that there exists a crossover point where the

velocity gradient changes sign. That point, the dividing line between the jet and slug, is the point of equal velocities described by Eichelberger, et al.

Applying the concept of a coalescent slug to our propagation model without further alteration it is seen to destroy the energy balance noted above. What is needed to restore this balance is the adjustment of the formation concept to allow formation of the <u>leading edge</u> of the slug at the position $\eta = 0$. The following table summarizes the two hypotheses.

<u>GARCIA</u>

$\eta = 0$	LE_j TE_{SL}	HIGH V_j LOW V_{SL}	TE_{SL} FORMED AT $\eta = 0$
$\eta = \eta_{MAX}$	TE_j LE_{SL}	LOW V_j HIGH V_{SL}	SLUG DISPERSIVE

<u>BROWN</u>

$\eta = 0$	LE_j LE_{SL}	HIGH V_j LOW V_{SL}	LE_{SL} FORMED AT $\eta = 0$
$\eta = \eta_{MAX}$	TE_j TE_{SL}	LOW V_j HIGH V_{SL}	SLUG COALESCENT

But, applying either hypothesis to the new model;

$$(18) \qquad (\hat{V}_{SL})_{\eta} < (\hat{V}_{SL})_{\eta+\Delta\eta}$$

Thus, from Equation (14)

$$(19) \qquad (V_D)_{\eta} \sin \left(\frac{\phi-\sigma}{2}\right)_{\eta} < (V_D)_{\eta+\Delta\eta} \sin \left(\frac{\phi-\sigma}{2}\right)_{\eta+\Delta\eta}$$

again for $(V_D)_\eta \approx (V_D)_{\eta+\Delta\eta}$:

$$(20) \qquad \sin\left(\frac{\phi-\sigma}{2}\right)_\eta < \sin\left(\frac{\phi-\sigma}{2}\right)_{\eta+\Delta\eta}$$

Combining inequalities 17 and 20;

$$(17) \qquad (\phi+\sigma)_\eta > (\phi+\sigma)_{\eta+\Delta\eta}$$

$$(20) \qquad (\phi-\sigma)_\eta < (\phi-\sigma)_{\eta+\Delta\eta}$$

leads to the conclusion that the spray angle σ is the important parameter when relating dispersion/coalescence effects of propagation to the kinematics of impact. In order for the inequalities to hold σ must decrease with increasing η.

Returning to Figure 10 an equality relationship can be seen between the incidence angle i_p and the spray angle σ. This relationship, derived mathematically by Garcia, is corroborated nicely by the hydraulic analogy of a water jet impinging on a flat smooth surface. This then links the significant parameter of dispersion, σ, to the geometrically defined convoluted surface. To control the dispersion/coalescence of the jet/slug one must control the angle between the convoluted surface and the plane of symmetry measured in the plane of the streamline that is perpendicular to the symmetry plane. The prediction then is that a "flattening out" of the two convoluted surfaces with increasing ξ will occur. This situation, depicted in Figure

23, is exactly that predicted by Sewell in Reference 1. The important dispersion variable then in terms of the input functions to the geometrical generation of the convoluted surface is the variation of acceleration across the vane (ζ as a function of η). The design variable of detonation wave shape can be seen to have significant influence on the impingement angle through contortion of the convoluted surface. A secondary design variable in the angle formation is the shape of the liner wall as stated previously. Reference 16 concerns a test program where some of these variables were arbitrarily altered in a conical shaped charge. The results of these tests (classified confidential) lend credance to the selection of these variables as significant. Detonation wave shaping is physically attainable by means of inert buffers, multi-point initiators, or lens charges with the latter method exhibiting the most flexibility. Maintenance of detonation wave shape throughout the length of the charge will probably require the imposition of a varience of deflagration rate with radius. This can be attained by means of a variable density of inerting ingredient.

Additional constraints are imposed on the design process by the dynamic yield strength of, and sonic (elastic wave) velocity in, the liner material. These limits are thoroughly explored and delineated by R.G.S. Sewell in Reference 17. The resulting limits on hydrodynamic jet formation, a function of liner velocity normal to the plane of symmetry,

are presented in terms of collapse angle and wall velocity. Given a particular value of detonation velocity these constraints translate into an upper and lower bound on the angle of incidence criterion of the optimization model presented here. This factor provides the only link with liner material properties necessary to dispersion/ coalescence control.

VI. CONCLUSION

A methodology has been presented that combines existing theory with a means of introduction of empirical data into a design process. Implementation of this approach is envisioned in several successive steps. A test program along the lines of that mentioned in Section V would be conducted utilizing the proposed liner material. These data would then be transformed into numerical form. Ideally, these fixed parametric functions would then be combined with the design variables in a computer program that provided a cathode ray tube display. The designer could then study the effect of variations in the design inputs and search for a solution that appears to offer a relatively constant value of i_p. This solution could then be refined by a machine solution for the angle at finite increments of ξ. A test specimen then built to the design values should provide some means for refinement of the process.

APPENDIX A

FEASIBILITY STUDY OF EXPERIMENTAL FUNCTION ANALYSIS

A. GENERAL

The work described herein was undertaken in support of the theoretical analysis that forms the main body of this thesis. The goals of this investigation were as follows:

1. To attempt to verify, in general, Sewell's description of the longitudinal variation in liner acceleration.
2. To attempt to identify the discontinuities in the instantaneous displacement of the liner by experimental means.
3. To determine whether or not the use of Sewell's approximation to the longitudinal wall displacement function entailed appreciable error.
4. To probe the feasibility of using similar but more sophisticated experimental means to accurately probe the ζ-ξ and ζ-η plane displacement functions under steady state detonation conditions.

The data base for this experiment was derived from pictures that were generated for a comparison study of LSC configurations by the Naval Weapons Test Center at China Lake, California. Their adaptation to this study was dictated by the lack of adequate explosive test facilities at NPS, as well as, the significant expense of such a test program. It

was felt that the data at hand, while marginal in many respects for this type of work, was adequate for the feasibility study proposed.

B. EXPERIMENTAL METHOD

A collage of framing camera photographs comprised of one full test run (shot #13) is presented as Figure 24. Examination of the first photograph (labeled zero) reveals the test setup utilized. An eight inch square piece of 1/8 inch mild steel was formed into the trough shape shown with a different included angle (2Θ) for each shot. Since the original purpose of this data was to investigate the effects of various outside corners or "star points" (see Figure 3) the explosive was placed inside the trough. A piece of 2" I.D. plastic pipe was cut to conform to the 2Θ angle, cemented to the steel, and the combination was butt-glued to a piece of 3/8" clear plexiglass. The resulting vessel was weighed, checked for volume, filled with Composition C-3 explosive, and then reweighed for charge density control. An electric detonator was then fitted to the charge and the steel painted a bright red for contrast with the background (original pictures are 35mm color). A thin black mylar tape was used to apply a one inch grid to the outside faces. Each charge was then mounted over a mirror inclined 45° to it's axis and a Cordin framing camera was oriented so as to combine side and end views in each picture. The framing camera was set to expose one frame per microsecond after charge initiation.

C. LIMITATIONS IMPOSED BY THE DATA

Despite the fact that the sighting plane minimizes edge effects, the charges used in acquiring these pictures were too small to guarantee their exclusion. Achievement of steady state detonation and the spherical nature of the detonation wave were not important due to the geometry of the camera sighting plane. Strangely enough, it was the mylar tape grid that most severely limited the experiment. Even under the extreme forces imposed, the mylar constrained the free surface of the steel enough to cause large periodic "holes" in the displacement curve. This effect is readily seen in Figures 25 and 26 which are samples of 54 such sheets used in the data reduction.

A further difficulty was brought into the picture by the choice of steel as the liner material. Carbon steel, and indeed, any alloy of iron, exhibits a phase change at a pressure of 190 Kbars. This phase change is accompanied by a sharp discontinuity in the Hugoniot curve at that point. This, of course, violates the constant plastic wave speed assumption of the reverberation time approach.

D. DATA REDUCTION

After many unsuccessful attempts by other means, the following sequence was used to "read" the instantaneous displacement curves:

1. The pictures were projected horizontally by a remote focusing projector a distance of 13 feet 4 inches

onto a flat vertical surface. A piece of 16" by 10" graph paper with a 0.1 inch grid was taped to the surface in such a way, that it could be moved and re-registered to each picture before tracing the outline of the liner free surface. The results are shown (typical values) in Fig. 25.

2. The graph paper was read with a magnifying glass describing the curve in hundredths of an inch every tenth of an inch as a table of digits.
3. The tabular values were plotted on semilog paper, thus expanding the displacement linearly while contracting the distance behind the detonation wave logarithmically [Fig. 26].
4. An attempt was made to correlate the discontinuities on the resulting curves with those predicted by Sewell's analysis and depicted in Figure 15.

Each step in the above process was undertaken as a separate series of independent value judgements to preclude the "manufacture" of favorable values. Attempts to differentiate the displacement curve to describe the velocity function were unsuccessful due to the large number of missing points caused by the mylar tape.

E. RESULTS AND CONCLUSIONS

The attempt to locate and fix the reverberation discontinuities was largely frustrated by the mylar tape effects. A measure of statistical correlation was exhibited

however that leads to the conclusion that the effects of the nonlinearities caused by the rapid change in properties of the liner when subjected to the shock pattern are such as to bring the liner displacement closer to Sewell's approximating function. The measure of repeatability in the curves seems to offer sufficient justification for use of a similar method to generate the input to a charge design program. A polynomial or exponential curve fit to such an empirically derived curve could successfully account for anomalies such as the phase change evidenced by steel liners.

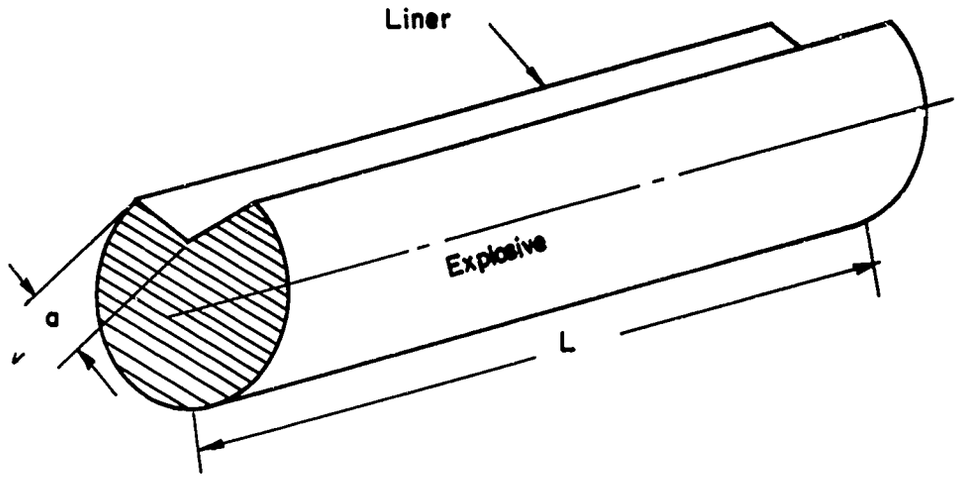

FIGURE 1. SIMPLE CONCEPTUAL MODEL OF THE LINEAR SHAPED CHARGE.

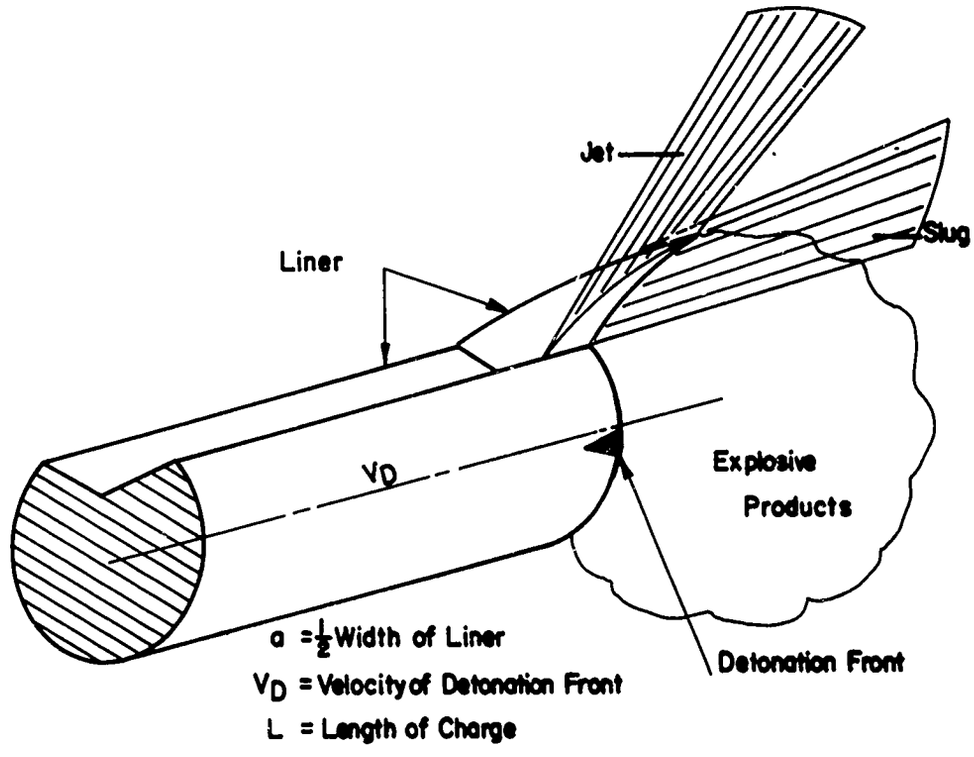

FIGURE 2. DETONATION PROCESS IN SIMPLE LINEAR SHAPED CHARGE.

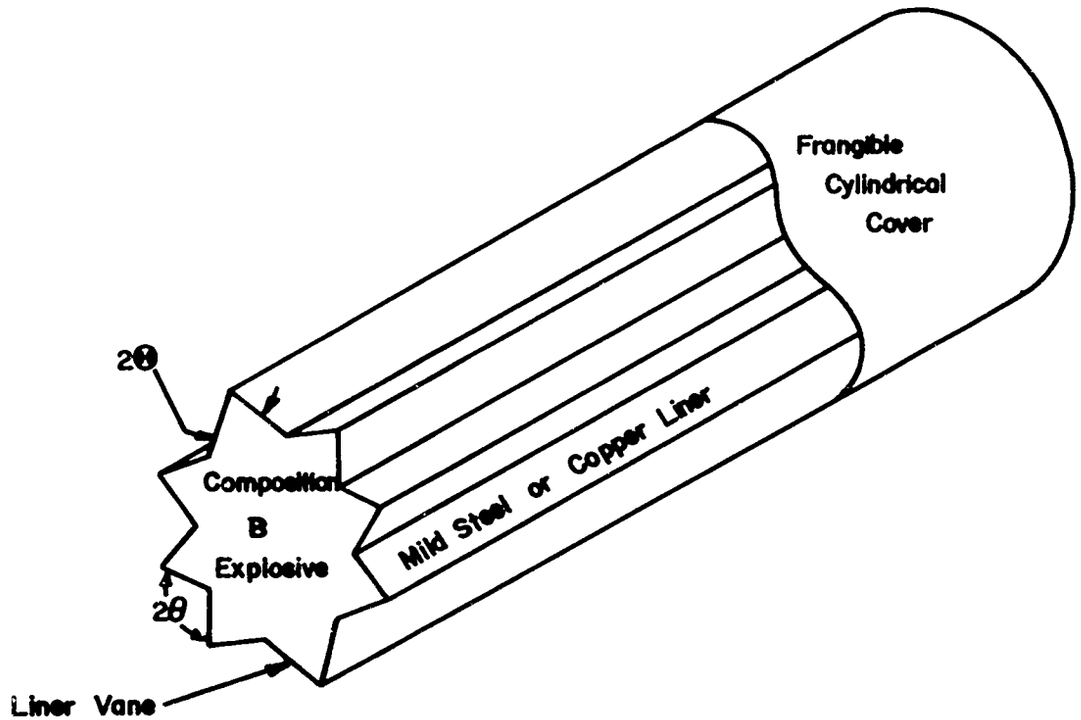

FIGURE 3. REPRESENTATIVE WARHEAD CONFIGURATION USING LSC PRINCIPLE

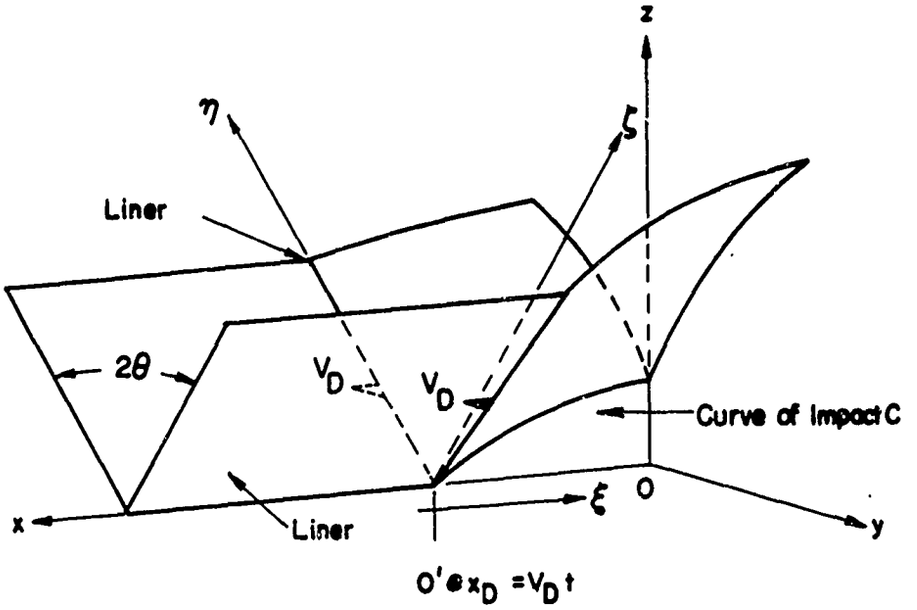

FIGURE 4. FIXED AND MOVING COORDINATE SYSTEMS

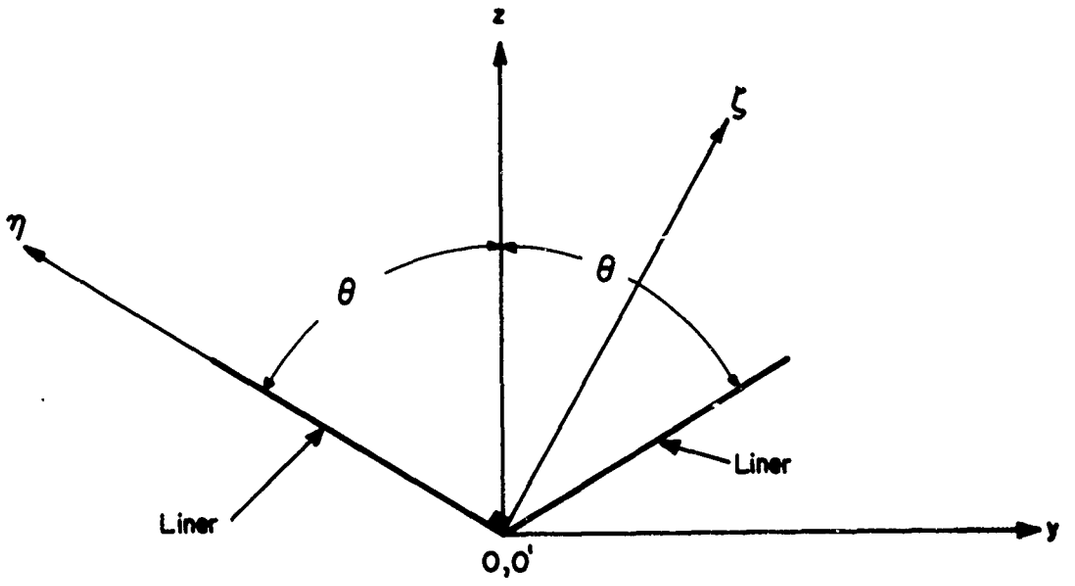

FIGURE 5. COORDINATES IN CROSS-SECTION COINCIDENT WITH DETONATION WAVEFRONT

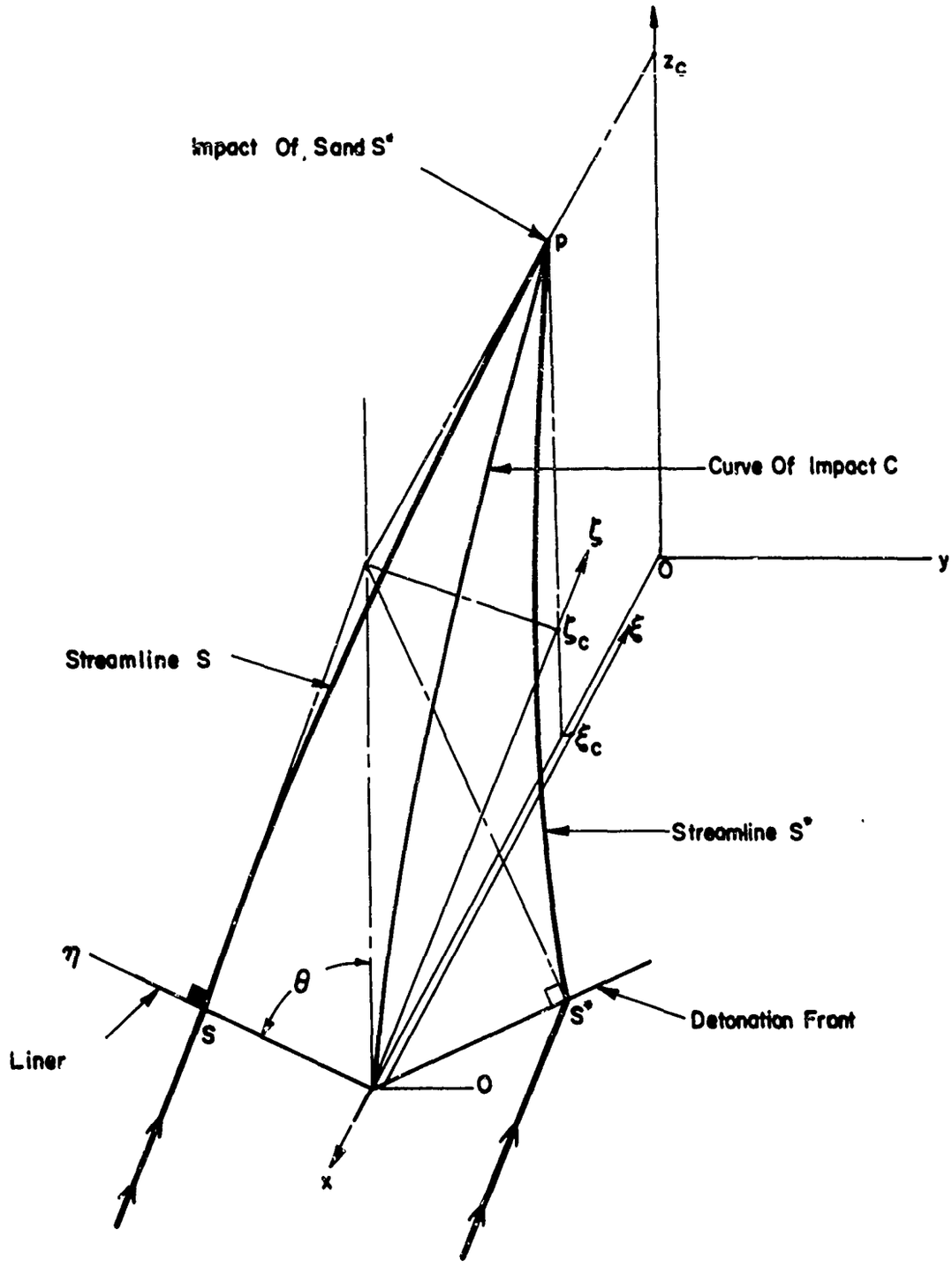

FIGURE 6. LINER FLOW AND STREAMLINE COORDINATES.

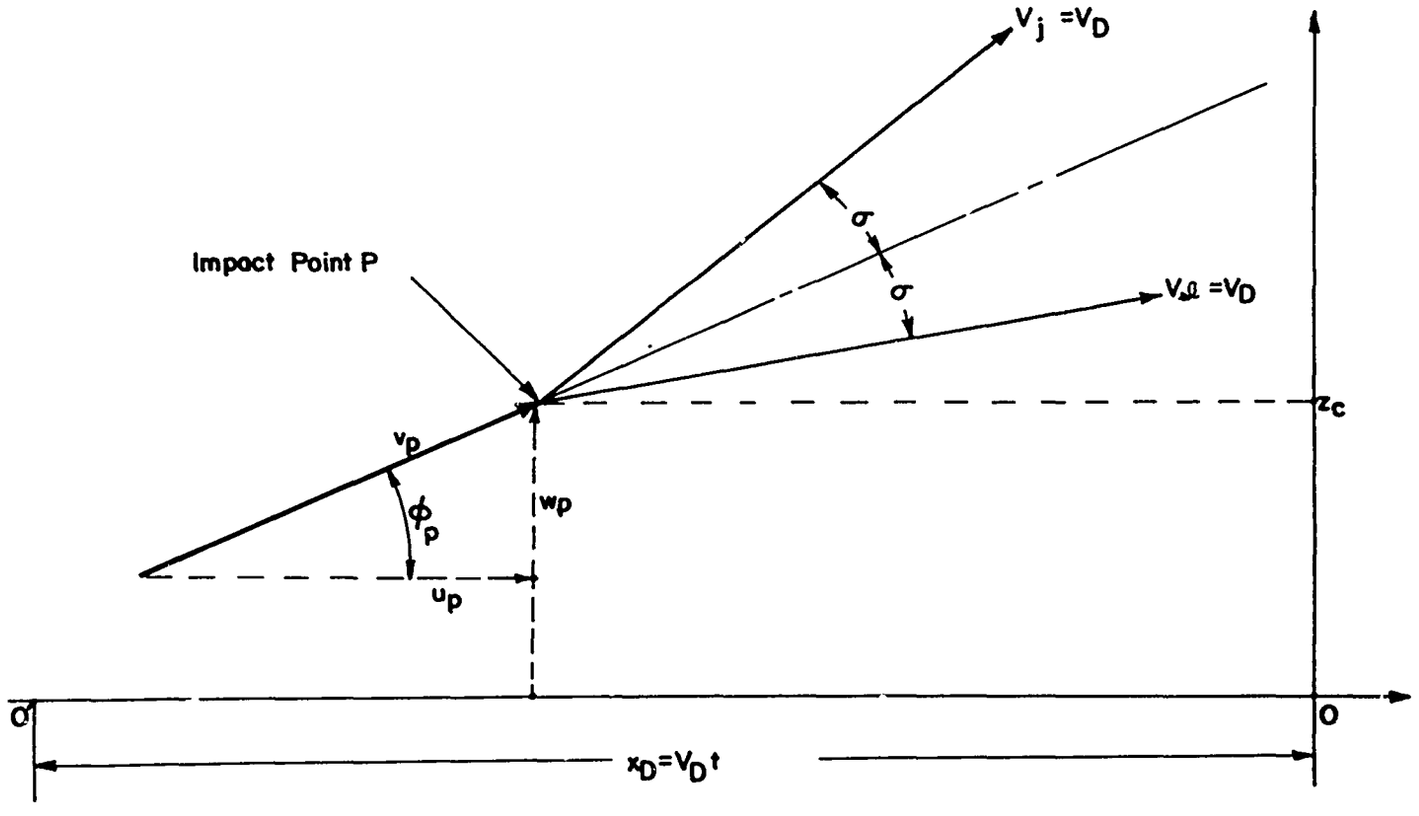

FIGURE 7. SEPARATION OF THE LINER STREAMLINE INTO JET AND SLUG STREAMLINES.

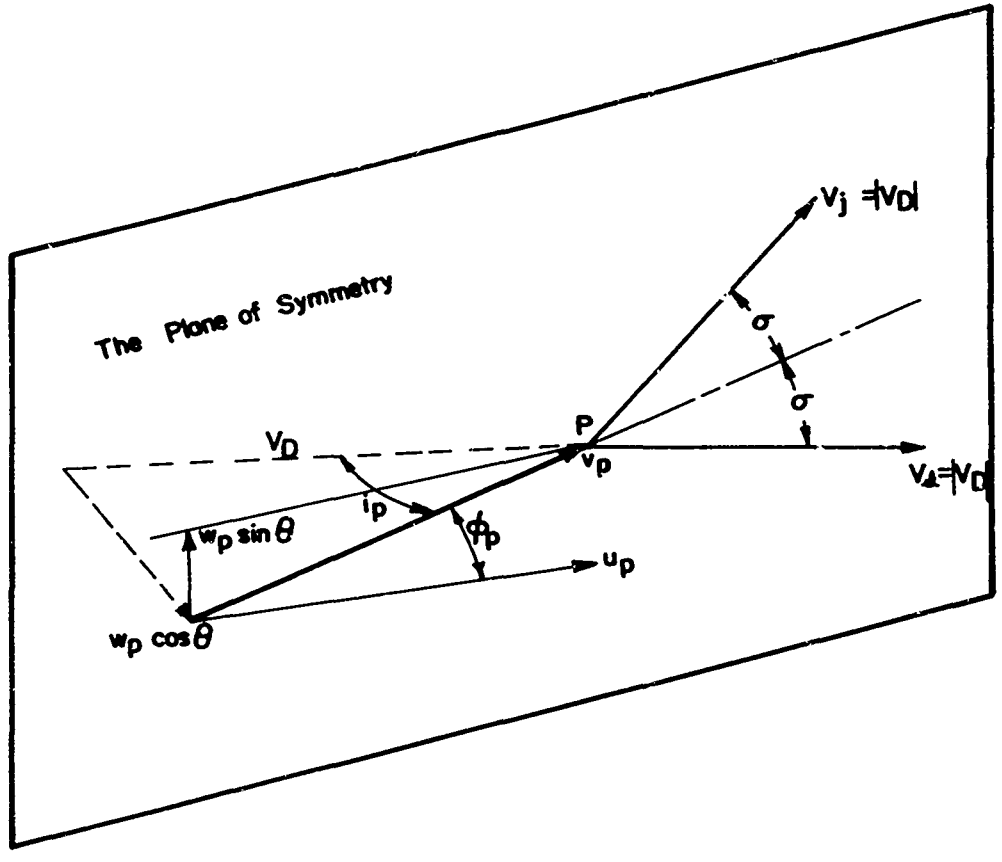

FIGURE 8. THREE-DIMENSIONAL KINETICS OF IMPACT.

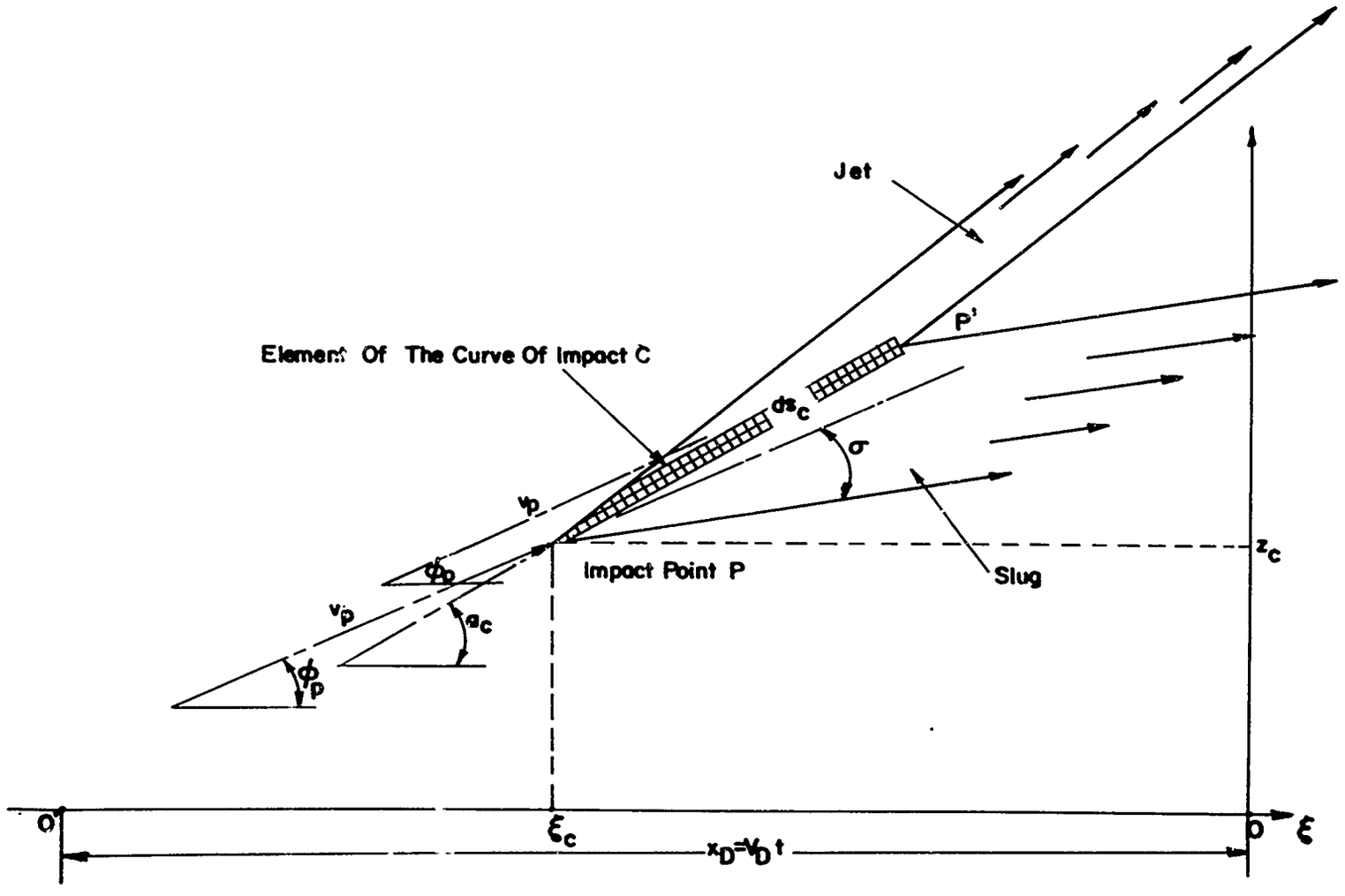

FIGURE 9. FORMATION OF THE JET AND SLUG ALONG A FINITE ELEMENT OF THE CURVE OF IMPACT.

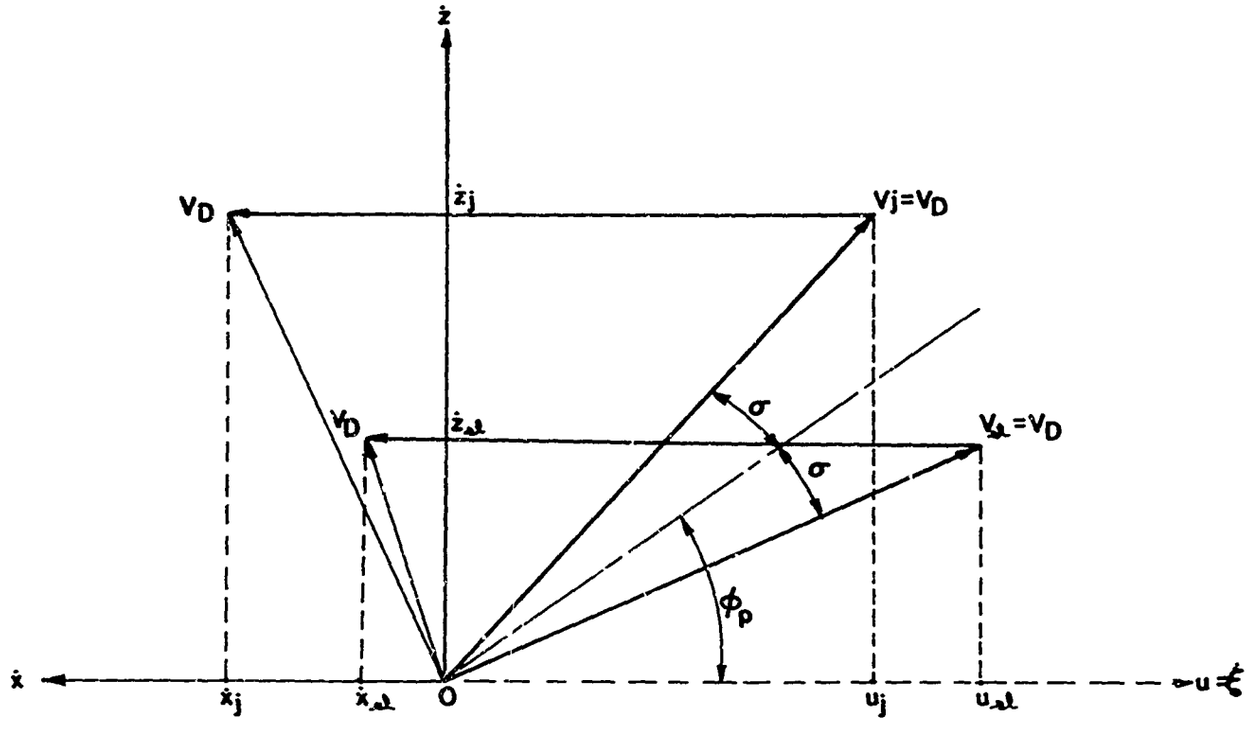

FIGURE 10. CONVERSION TO INERTIAL VELOCITIES

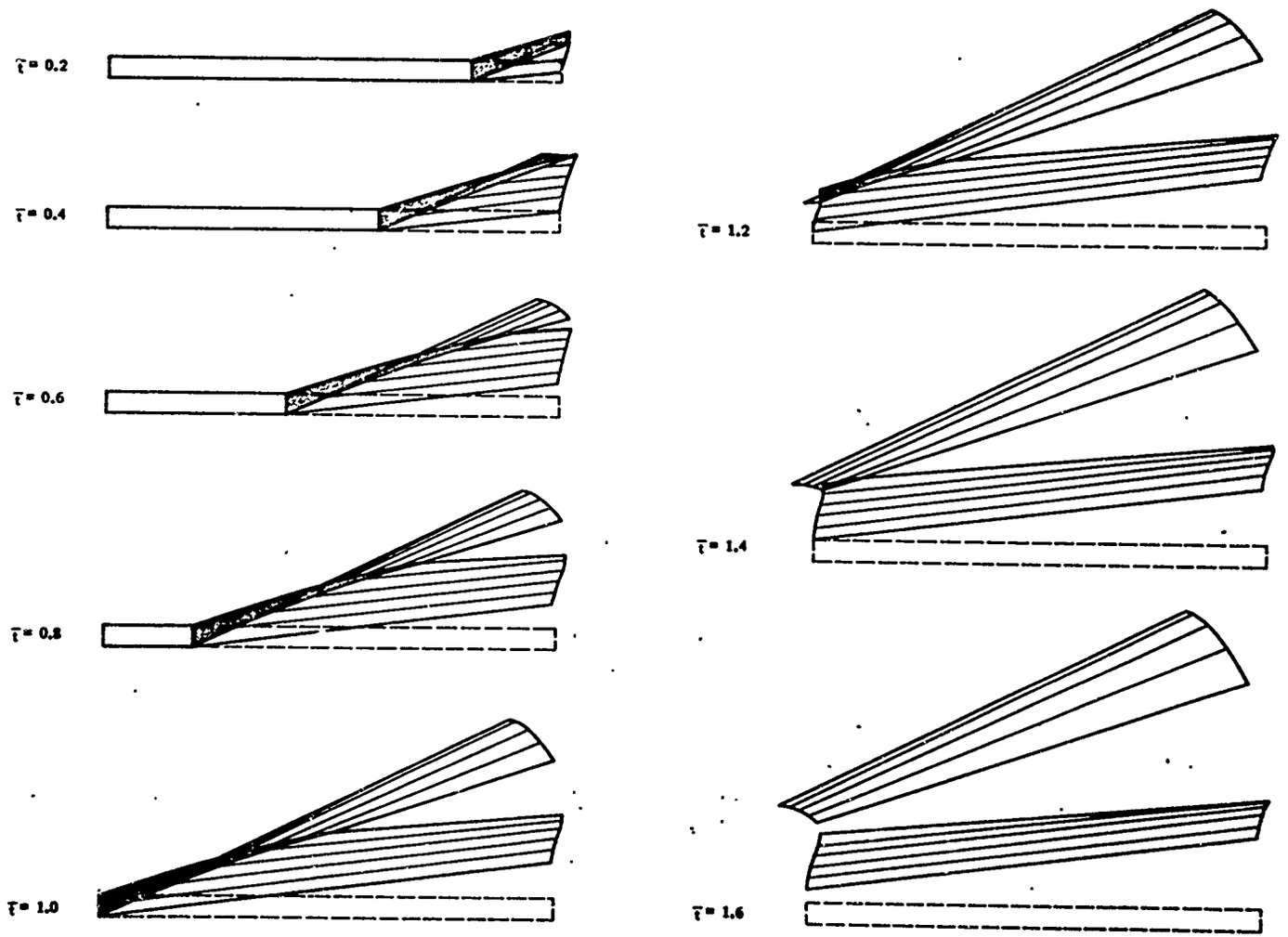

FIGURE 11 SEQUENTIAL DEVELOPMENT OF JET AND SLUG

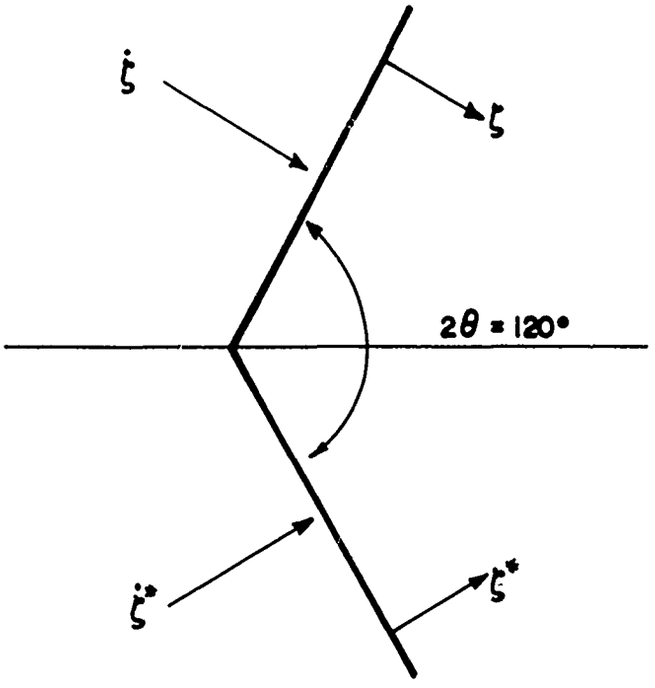

FIGURE 12. CONSTANT ANGLE IDEALIZED COLLAPSE CASE.

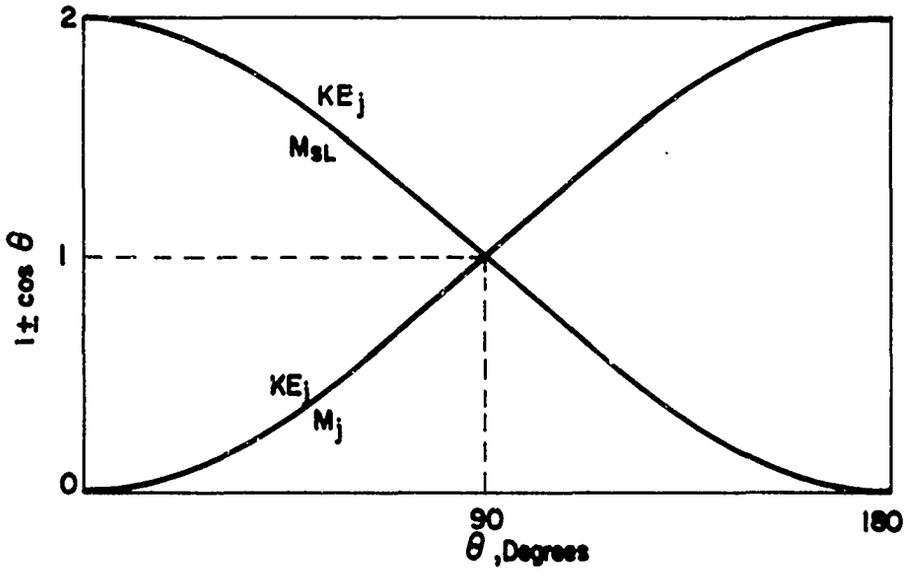

FIGURE 13. BALANCE BETWEEN MASS AND KINETIC ENERGY DIVISION FOR THE IDEALIZED COLLAPSE CASE.

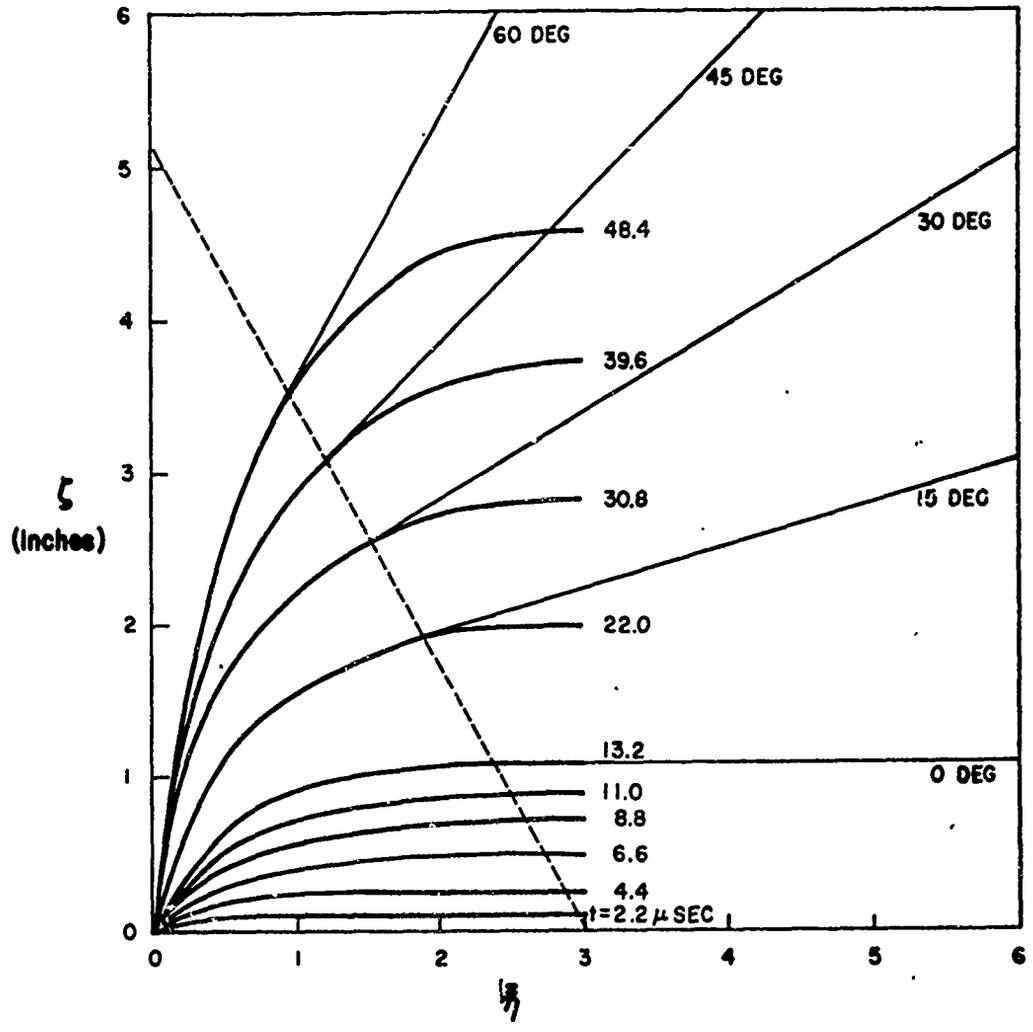

FIGURE 14. DISPLACEMENT HISTORY ACROSS THE VANE

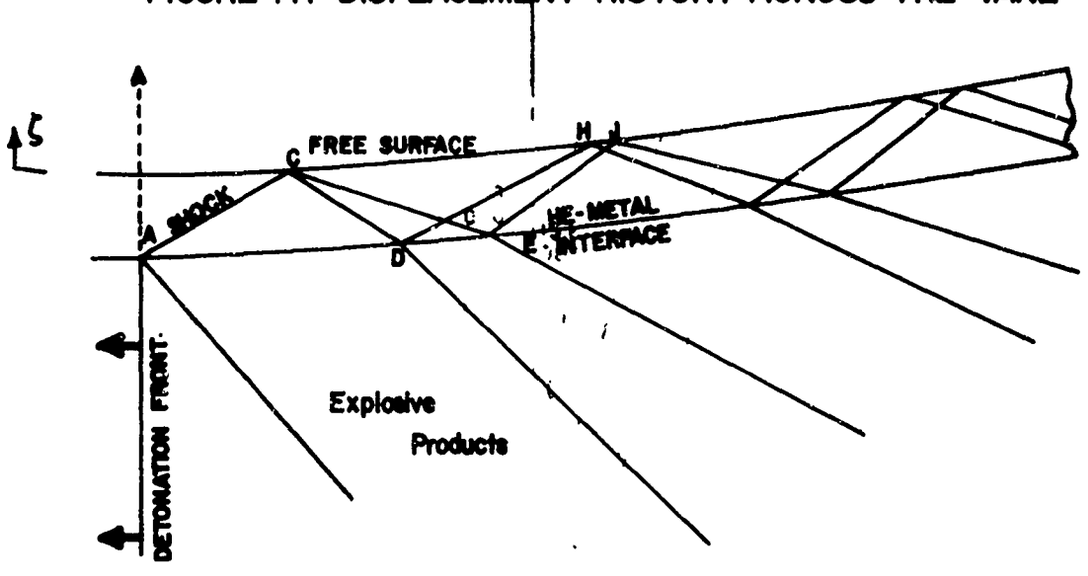

FIGURE 15. SHOCK WAVE INTERACTION BEHIND THE DETONATION FRONT

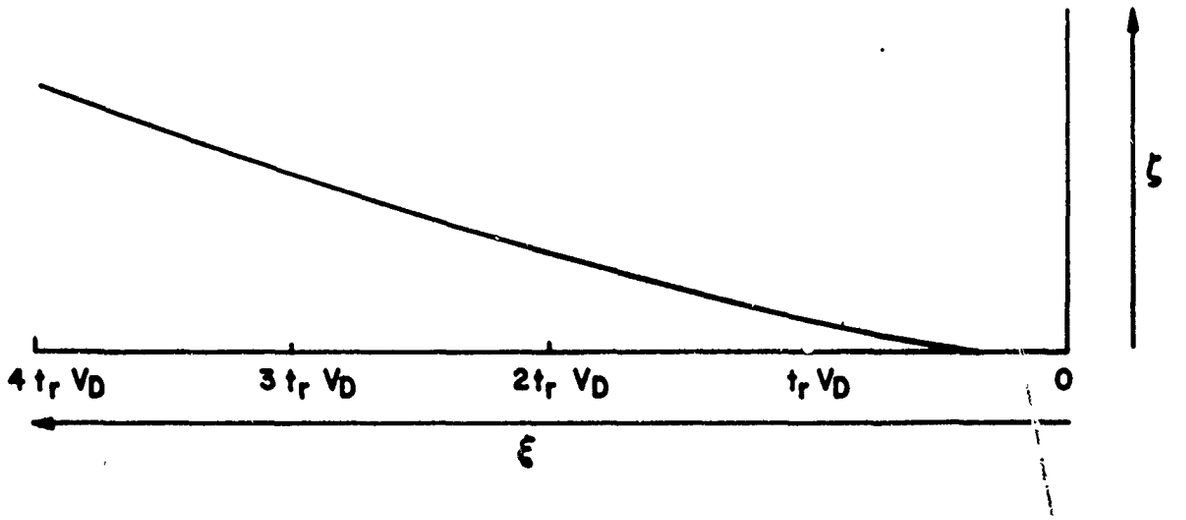

FIGURE 16. LINER DISPLACEMENT AS AFFECTED BY LONGITUDINAL ACCELERATION VARIATION (APPROXIMATING FUNCTION)

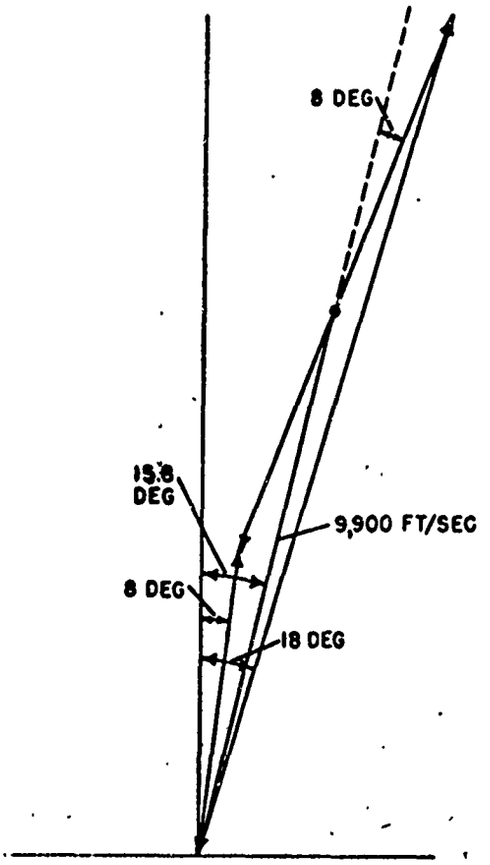

FIGURE 17. SUMMATION OF VELOCITY VECTORS

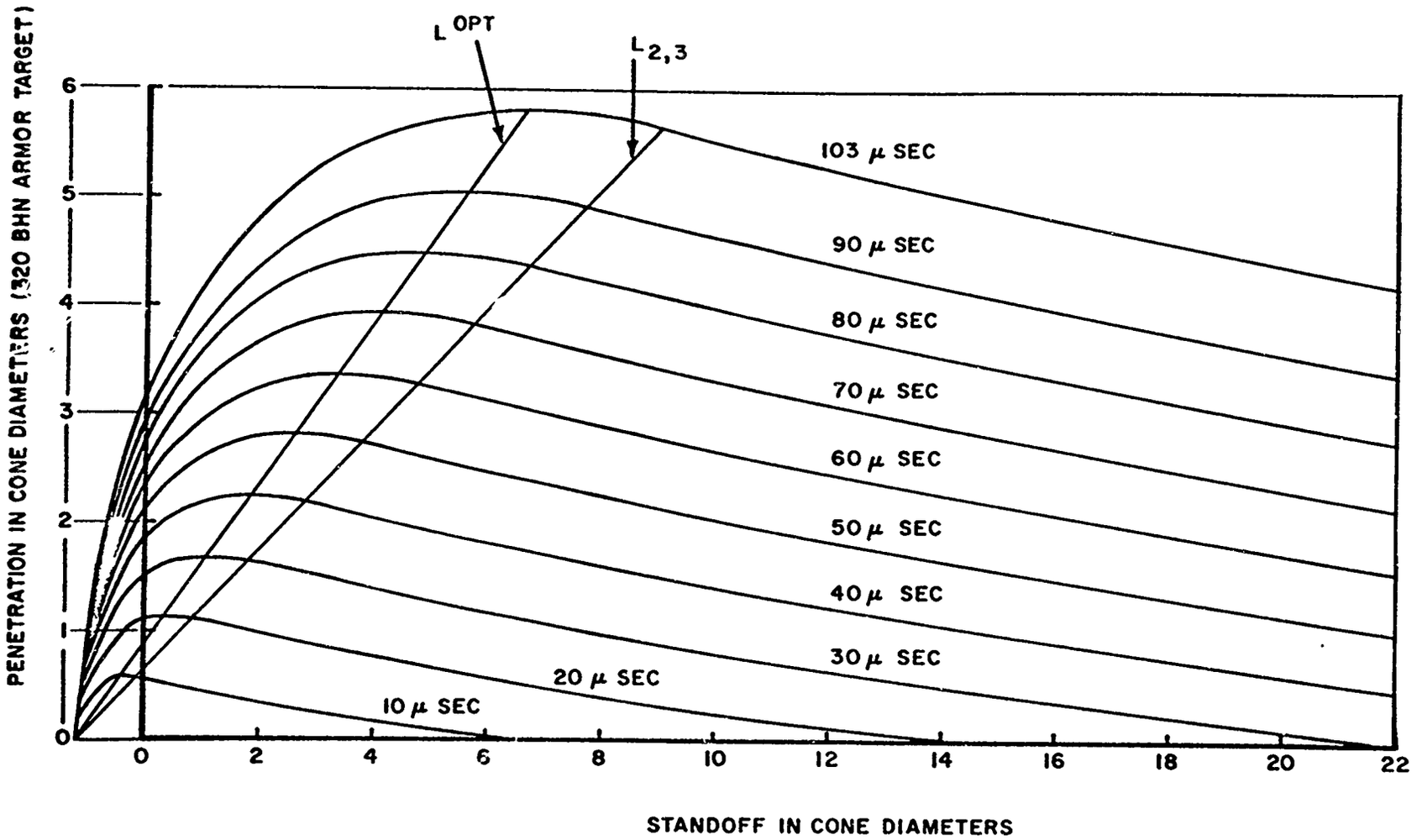

FIGURE 18 PENETRATION-STANDOFF CURVES FOR VARIOUS VALUES OF JET BREAKUP TIME (CONICAL SHAPED CHARGE)

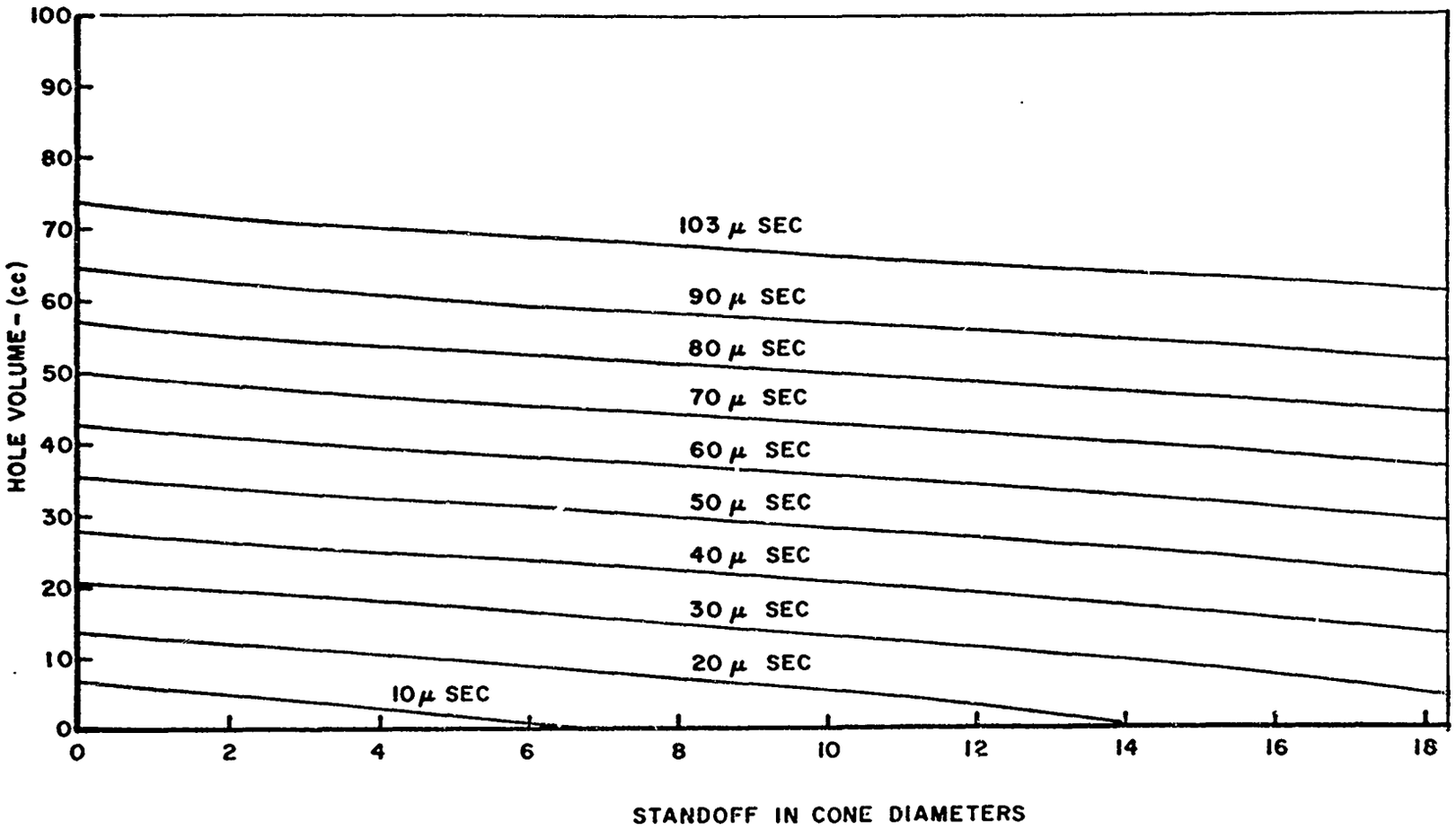

FIGURE 19 HOLE VOLUME-STANDOFF CURVES FOR VARIOUS VALUES OF JET BREAKUP TIME (CONICAL SHAPED CHARGE)

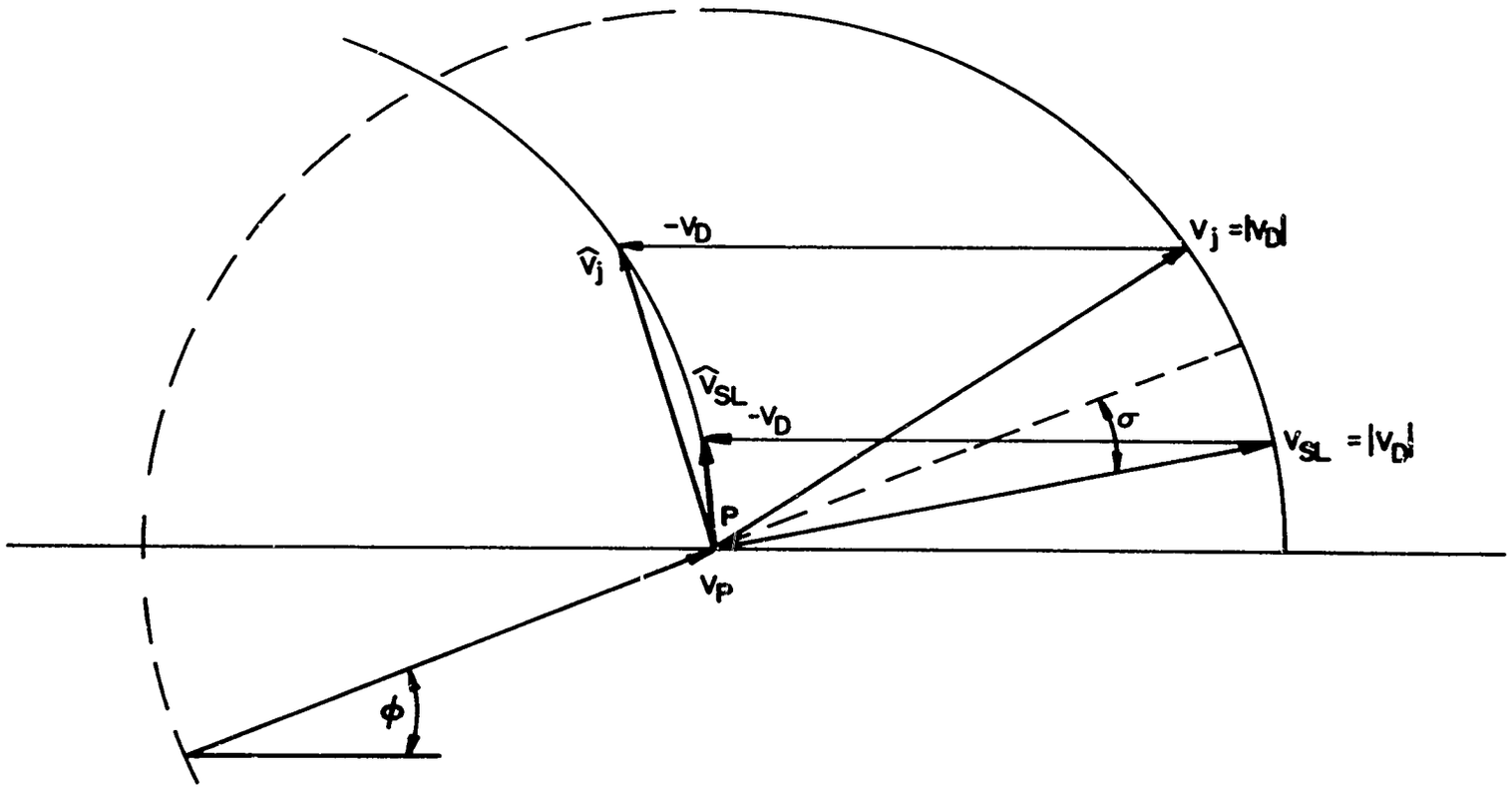

FIGURE 20. LOCI OF POSSIBLE VELOCITY SOLUTIONS

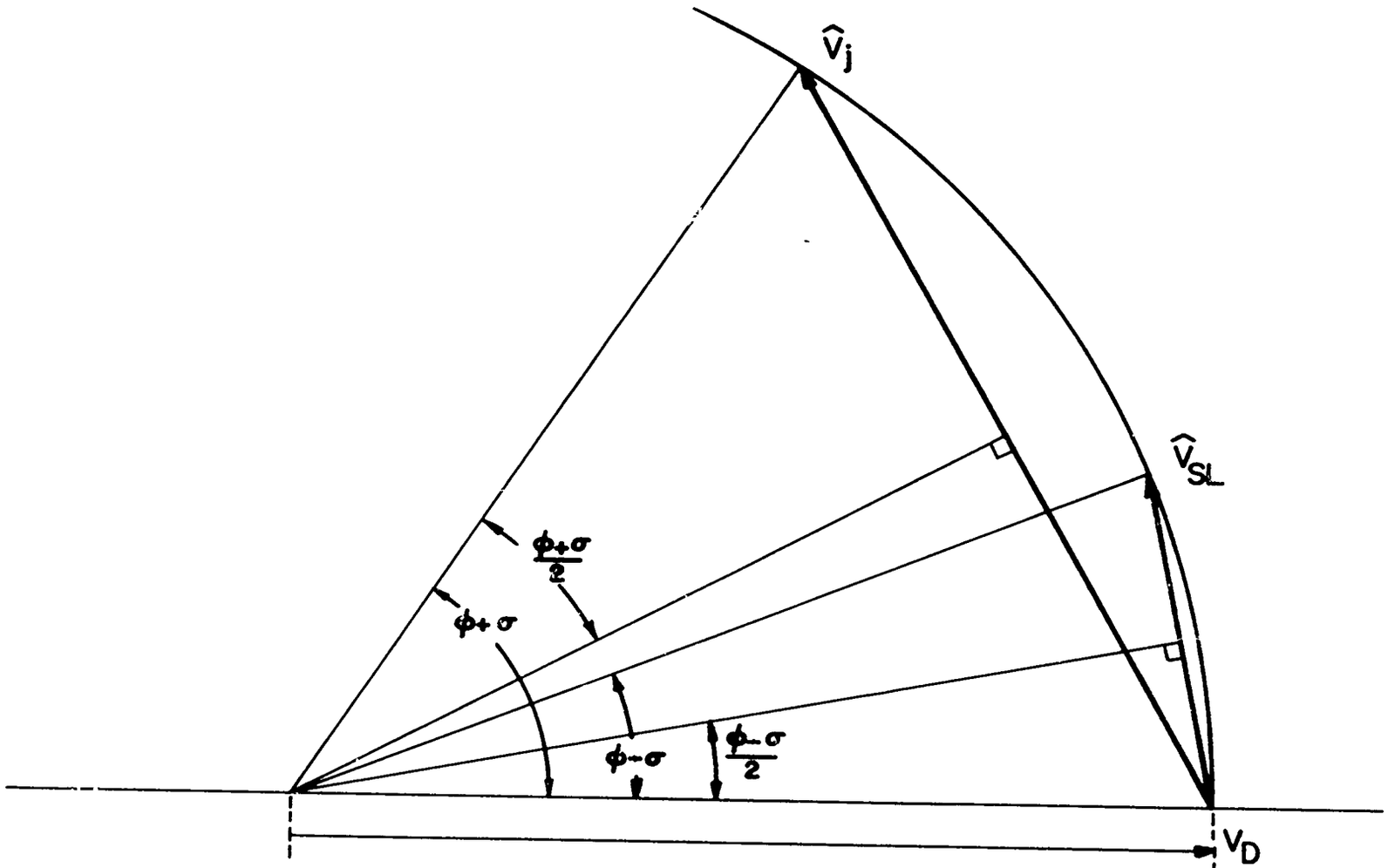

FIG. 21 GEOMETRY OF INERTIAL VELOCITY SOLUTIONS

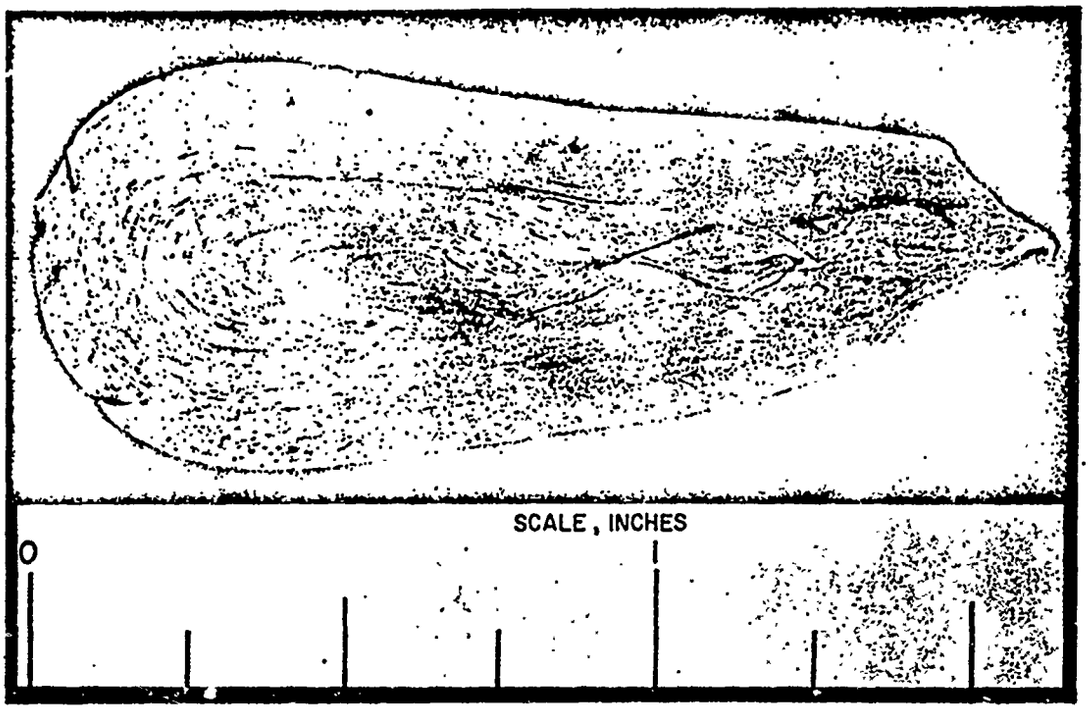

FIGURE 22. SECTION OF RECOVERED SLUG FROM LINEAR SHAPED CHARGE OF MILD STEEL.

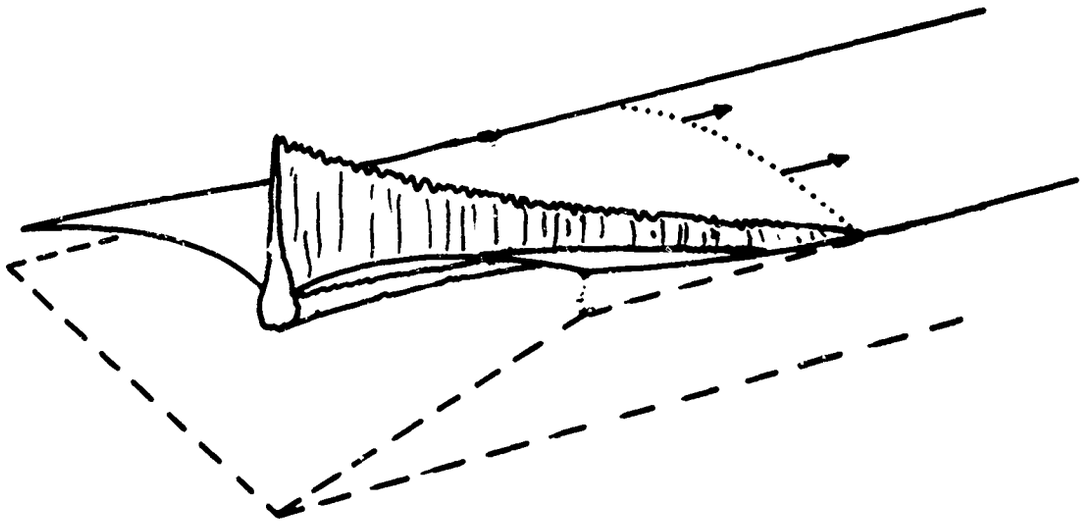

FIGURE 23. GENERAL SHAPE OF THE CONVOLUTED SURFACES FOR THE CASE OF A NEARLY PLANE DETONATION WAVE.

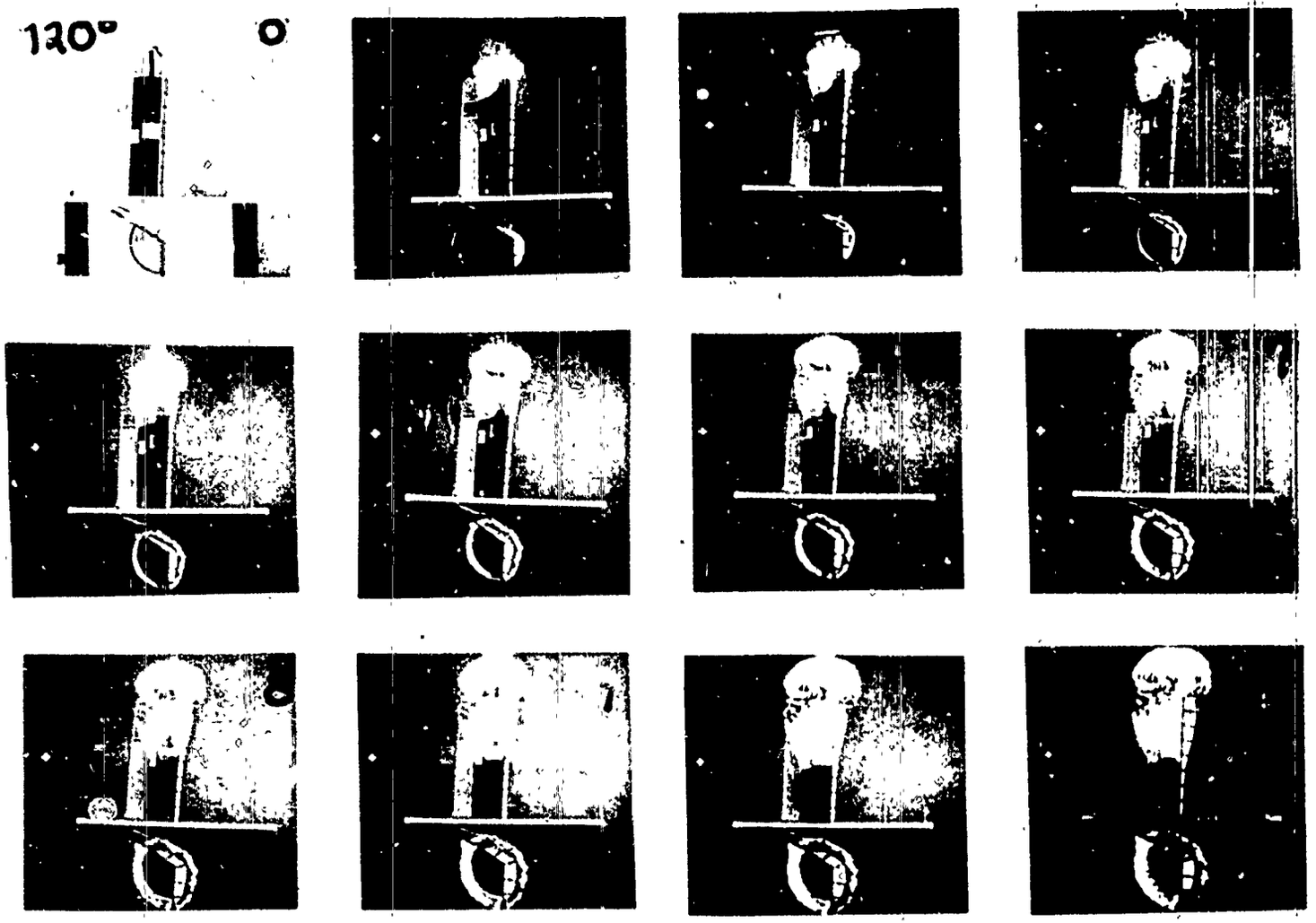

FIGURE 24. FRAMING CAMERA RECORD OF THE DETONATION OF THE TEST MODEL.

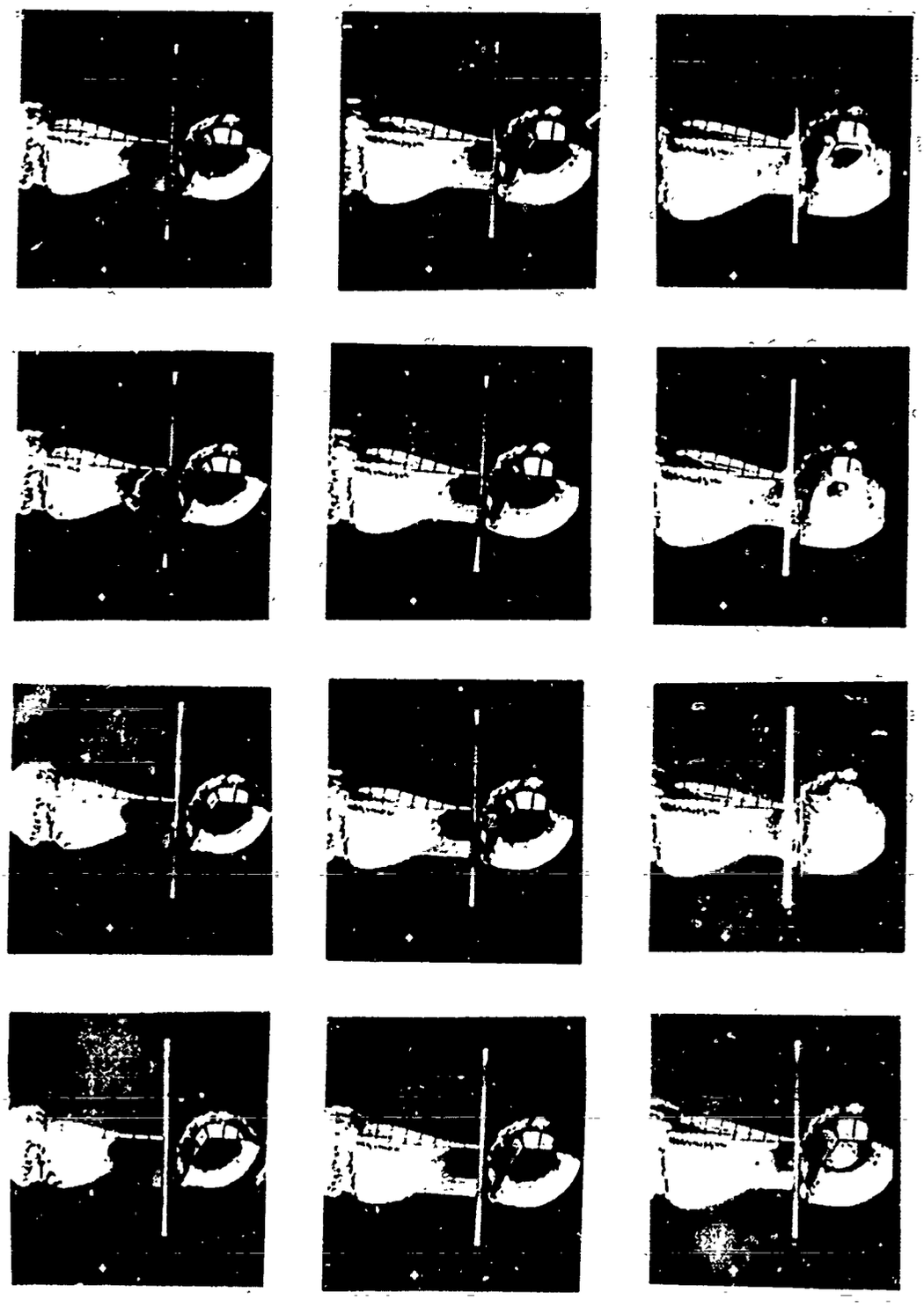

FIGURE 24. (Continued)

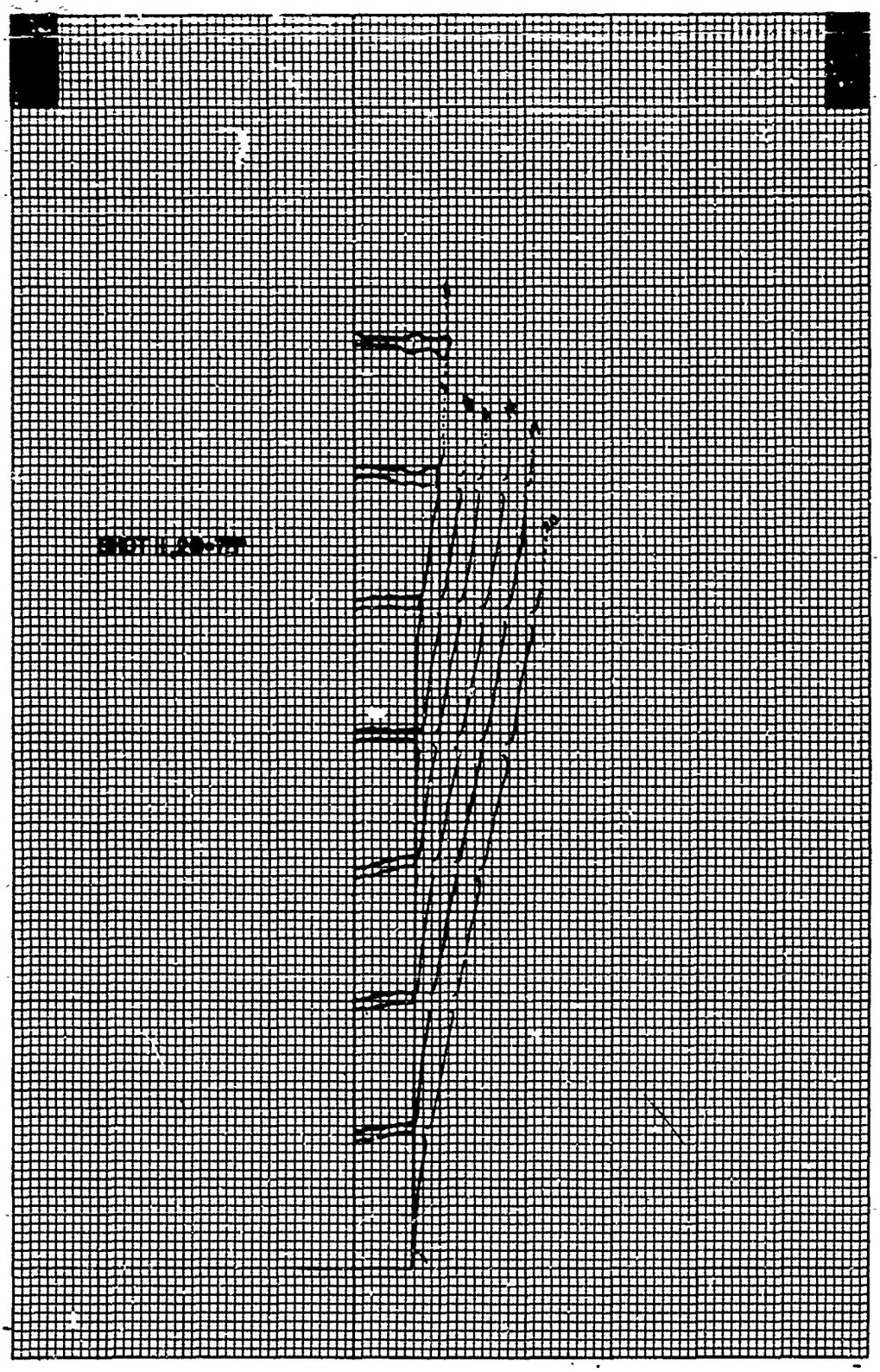

FIGURE 25. TRACING OF LINER FREE SURFACE DISPLACEMENT CURVES (TYPICAL).

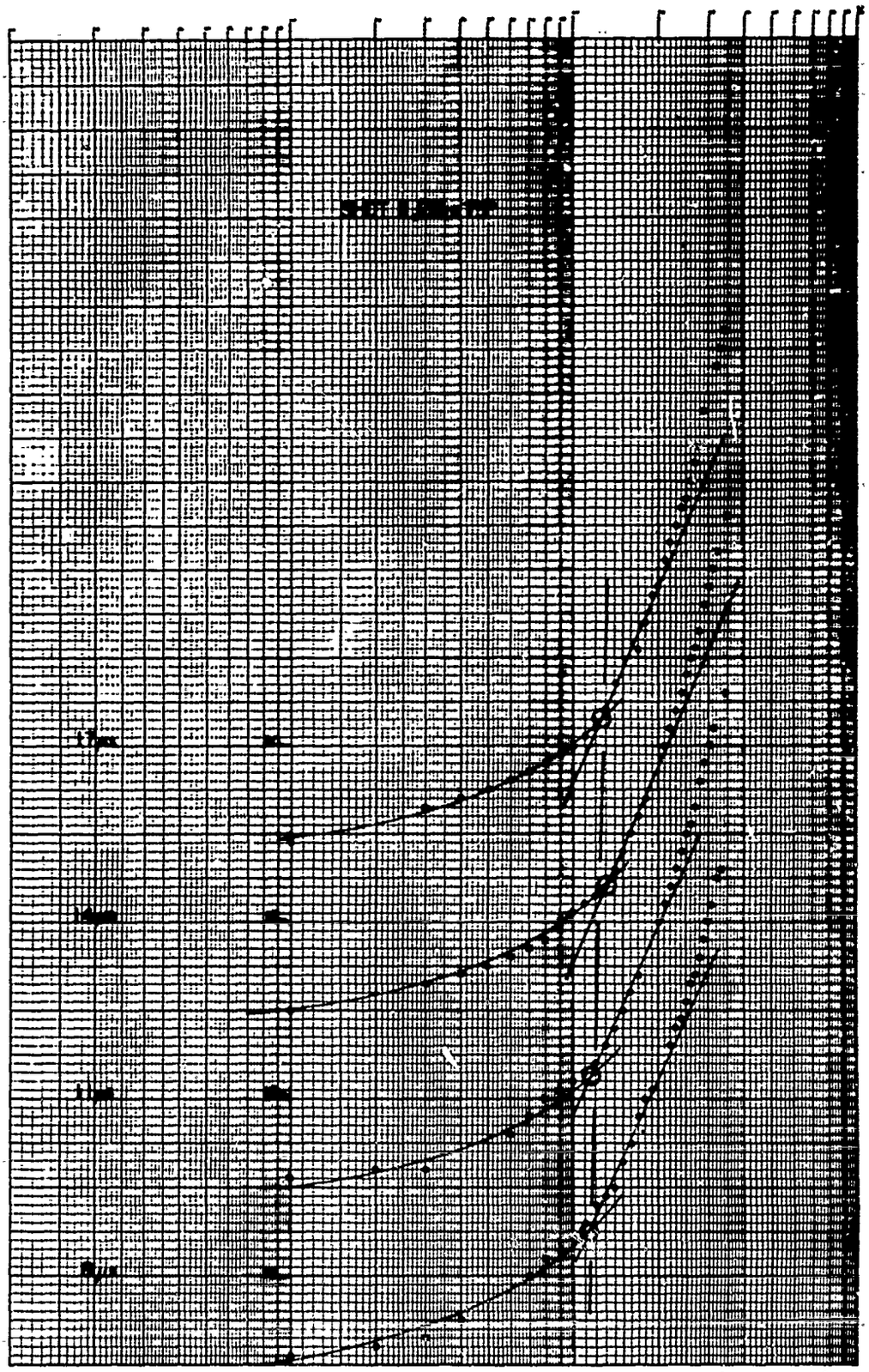

FIGURE 26. EXPANDED PLOT USED IN LOCATION OF FREE SURFACE DISCONTINUITIES (TYPICAL).

REFERENCES

1. Sewell, R.G.S., The Collapse Process of the End-Initiated Linear Shaped Charge, Naval Weapons Center, China Lake, California, August 1965.

2. Naval Missile Center Report TM-67-64, The End-Initiated Linear Shaped Charge: An Analytical Model, by M.A. Garcia, 1 December 1967.

3. Ballistic Research Lab Report 405, The Initial Velocities of Fragments from Bombs, Shells and Grenades, R.W. Gurney, 14 September 1943.

4. NAVWEPS Report 7592, Table of Initial Fragment Velocities Calculated from Gurney and Sterne Formulas for Various C/M Ratios and Explosive Energies, J.A. Weeks, 22 December 1960.

5. Ballistic Research Lab Report 1296, Penetration of Shaped-Charge Jets into Metallic Targets, R. DiPersio, J. Simon, A.B. Merendino, September 1965.

6. Ballistic Research Lab Report 1313, Theory of Residual Penetration by Ideal Shaped Charge Jets, R. DiPersio, J. Simon, March 1966.

7. Ballistic Research Lab Report MR-1897, The Effect of Jet Breakup Time on the Penetration Performance of Shaped Charges, R. DiPersio, J. Simon, January 1968.

8. Ballistic Research Lab Report MR-1542, The Penetration-Standoff Relation for Idealized Shaped-Charge Jets, R. DiPersio, J. Simon, February 1964.

9. Naval Ordnance Test Station TP 3327, Walleye Warhead Analysis; Jet Effectiveness Against Various Tactical Targets (U), E. Breitenstein, March 1964, Classified Confidential.

10. Naval Ordnance Test Station TP 3476, Walleye Warhead Analysis; Effectiveness Against Light Bridges (U), Astro Technology Corp., February 1964, Classified Confidential.

11. Naval Ordnance Test Station TP 3624, A Study of the Walleye Warhead Effectiveness (U), R. Smith, D. Davis, August 1964, Classified Confidential

12. Naval Ordnance Test Station TP 2958, A Large Linear Shaped Charge Warhead (U), P. Cordle, M. McCubbin, September 1962, Classified Confidential.

13. Naval Ordnance Test Station TP 3301, Linear Shaped Charge Study (U), E. O'Connor, August 1963, Classified Condifential

14. Pugh, E. M., Eichelberger, R. J., and Rostoker, N., "Theory of Jet Formation by Charges with Lined Conical Cavities," Journal of Applied Physics, V. 23, pp.532-536, May 1952.

15. Eichelberger, R. J., and Pugh, E. M., "Experimental Verification of the Theory of Jet Formation by Charges with Lined Conical Cavities," Journal of Applied Physics, V. 23, pp. 537-542, May 1952.

UNCLASSIFIED

Security Classification

DOCUMENT CONTROL DATA - R & D

(Security classification of title, body of abstract and indexing annotation must be entered when the overall report is classified)

1. ORIGINATING ACTIVITY (Corporate author)	2a. REPORT SECURITY CLASSIFICATION
Naval Postgraduate School Monterey, California 93940	Unclassified
	2b. GROUP

3. REPORT TITLE

A NEW OPTIMIZATION THEORY FOR THE END-INITIATED LINEAR SHAPED CHARGE

4. DESCRIPTIVE NOTES (Type of report and inclusive dates)

Master's Thesis; October 1969

5. AUTHOR(S) (First name, middle initial, last name)

George Elliott Brown, Jr., Lieutenant, United States Navy

6. REPORT DATE	7a. TOTAL NO. OF PAGES	7b. NO. OF REFS
October 1969	66	15

8a. CONTRACT OR GRANT NO.	9a. ORIGINATOR'S REPORT NUMBER(S)
b. PROJECT NO.	
c.	9b. OTHER REPORT NO(S) (Any other numbers that may be assigned this report)
d.	

10. DISTRIBUTION STATEMENT

This document has been approved for public release and sale; its distribution is unlimited.

11. SUPPLEMENTARY NOTES	12. SPONSORING MILITARY ACTIVITY
	Naval Postgraduate School Monterey, California 93940

13. ABSTRACT

An exposition of the two existing analytical approaches to the end initiated linear shaped charge is made. After a theory is put forth relating optimizaiton to increased energy transfer at increased standoff distances, this effect is linked to the dispersive nature of the jet mass. An analytical design approach is then formulated that combines elements of both existing models. The object of this approach is to integrate experimental data into a mathematically definitive analysis. A theoretical link is then developed between the dispersive nature of the jet and the design input parameters, thus completing the optimization model.

DD FORM 1 NOV 68 1473 (PAGE 1)

S/N 0101-807-6811

Security Classification

A-31408

14 KEY WORDS	LINK A		LINK B		LINK C	
	ROLE	WT	ROLE	WT	ROLE	WT
LINEAR SHAPED CHARGE						
WARHEAD						
EXPLOSIVE CUTTING						